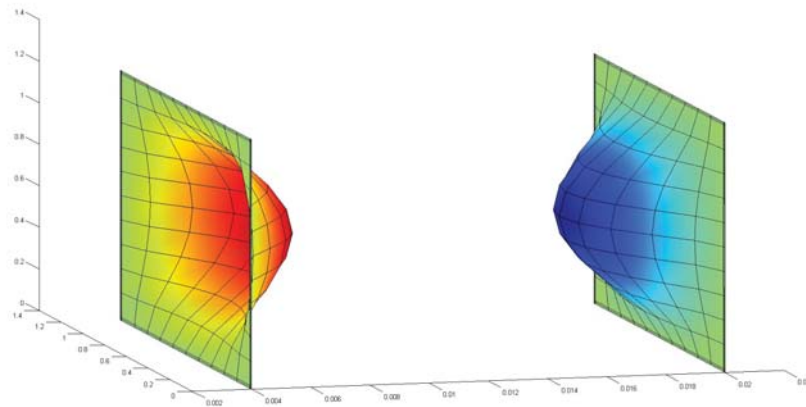




**LUND**  
UNIVERSITY



# COMPUTATIONAL METHOD FOR BULGING IN INSULATING GLASS UNITS

DANIEL SVENSSON

Structural  
Mechanics

*Master's Dissertation*



DEPARTMENT OF CONSTRUCTION SCIENCES  
DIVISION OF STRUCTURAL MECHANICS

ISRN LUTVDG/TVSM--15/5206--SE (1-59) | ISSN 0281-6679

MASTER'S DISSERTATION

# COMPUTATIONAL METHOD FOR BULGING IN INSULATING GLASS UNITS

DANIEL SVENSSON

Supervisors: Professor **KENT PERSSON**, Div. of Structural Mechanics, LTH.

Examiner: **JONAS LINDEMANN**, PhD, Div. of Structural Mechanics, LTH & Lunarc, Lund.

Copyright © 2015 Division of Structural Mechanics  
Faculty of Engineering (LTH), Lund University, Sweden.

Printed by Media-Tryck LU, Lund, Sweden, June 2015 (*PI*).

**For information, address:**

Div. of Structural Mechanics, LTH, Lund University, Box 118, SE-221 00 Lund, Sweden.

Homepage: <http://www.byggmek.lth.se>



## **Preface**

This master dissertation was carried out at the Division of Structural Mechanics at Lund University. I would like to thank my supervisor Professor Kent Persson who helped me throughout this work and was always available when I needed guidance.

This thesis is the end of five fantastic years of studies at Lund University. I would like to thank my family and friends for your support during my education.

Lund, June 2015.

Daniel Svensson



## Abstract

An insulating glass unit (IGU) normally consists of two or three glass panes which are separated by a spacer. The spacer creates a cavity between the glass panes which is filled with a gas to increase the insulating capacity of the IGU. To keep the gas in the cavity and to stop vapor from getting in, the cavity has to be hermetically sealed. This makes the IGU sensitive to pressure change and volume change which may occur if the unit is subjected to temperature changes, changes in ambient pressure or lateral loads such as wind loads. Any of these load cases will inflict a change in the gas pressure that changes the cavity volume. When the gas pressure changes the glass panes will bulge and stresses will occur.

To study this problem a computational method was created with the finite element method. In the method, was a three dimensional model created to calculate the displacement and the stress in the glass that occurs when the unit is subjected to various loads. The computational method handles different dimensions of the IGU but is restricted to rectangular shapes. The method uses the ideal gas law to find the solution by iterations.

FE-models were also created in Abaqus to evaluate the developed method for different dimensions and load cases. The Abaqus model used hydrostatic fluid elements to represent the gas in the cavity. The difference between the Abaqus model and the computational method was small and a difference of 8% was the largest when comparing displacements.

The computational method was also compared with the results from the master thesis made by Martin Andersson and Simon Nilsson, who made experimental tests and FE-analyzes of insulating glass units subjected to temperature change. The developed method had a difference of 2-5 mm in comparison with the experimental results, which was similar to the difference between the experimental results and their FE-analysis.



## Sammanfattning

Isolerglas består normalt av två eller tre separerade glasrutor. Mellan dessa skapas en kavitet som består av en fyllnadsgas för att öka den isolerande förmågan hos enheten. Kaviteten måste vara försluten för att gasen inte ska sippra ut och för att förhindra att fukt ska trängas in i kaviteten. Detta gör att ett isolerglas är känsligt för tryck- och volymändring som kan uppstå om den blir utsatt för temperaturändring, ändring i omgivande tryck eller om en yttre last, så som vindlast, belastar isolerglasenheten. Om isolerglaset blir utsatt för något av dessa laster kommer en tryckändring ske i gasen samt att kavitetens volym kommer att ändras. En volymändring ger upphov till att glaset i isolerglasenheten får en deformation. Om gastrycket och kavitetsvolymen ändras kommer glaset att buktas och spänningar uppstår i glaset.

För att lösa det problemet utvecklades en beräkningsmetod med hjälp av finita elementmetoden. En tredimensionell isolerglasmodell skapades och förskjutningar och spänningar i glaset kan beräknas då isolerglasets utsätts för olika lastfall. Beräkningsmetoden beräknar detta för olika dimensioner men är begränsad till rektangulära geometrier. I metoden används den ideala gaslagen för att iterera fram en lösning.

En finita elementmodell skapades även i beräkningsprogrammet Abaqus för att utvärdera den utvecklade beräkningsmetoden för olika dimensioner och lastfall. Skillnaden mellan Abaqus-modellen och beräkningsmetoden var liten och den största skillnaden i förskjutning uppgick till 8%.

Beräkningsmetoden jämfördes också med resultat från ett tidigare examensarbete av Martin Andersson och Simon Nilsson. I det examensarbetet utfördes experimentella tester och finita elementanalyser på isolerglas utsatta för temperaturvariation. Förskjutningen från beräkningsmetoden visade nästan samma resultat som deras finita elementanalys och båda metoderna visade en skillnad på 2-5 mm jämfört med de experimentella testerna.



# Contents

<b>1</b>	<b>Introduction</b>	<b>1</b>
1.1	Background . . . . .	1
1.2	Objective, aim and method . . . . .	1
1.3	Limitation . . . . .	2
1.4	Outline . . . . .	2
<b>2</b>	<b>Insulating glass unit</b>	<b>5</b>
2.1	Earlier studies . . . . .	5
2.2	IGU structure . . . . .	9
2.2.1	Glass . . . . .	9
2.2.1.1	Float glass . . . . .	10
2.2.1.2	Types of glass . . . . .	10
2.2.1.3	Mechanical properties of glass . . . . .	11
2.2.2	Spacer and sealants . . . . .	12
2.2.2.1	Primary sealant . . . . .	13
2.2.2.2	Secondary sealant . . . . .	13
2.3	Cavity . . . . .	14
<b>3</b>	<b>Theory</b>	<b>15</b>
3.1	Ideal gas in enclosed cavity . . . . .	15
3.1.1	Initial conditions for the gas . . . . .	16
3.2	Load cases . . . . .	16
3.3	Finite element method . . . . .	17
3.3.1	General . . . . .	17
3.3.2	Elements . . . . .	18
3.3.3	Linear elasticity . . . . .	19
3.3.4	Element load . . . . .	20
3.4	Interaction between gas and structure . . . . .	20

3.4.1	Volume change . . . . .	20
3.4.2	Stiffness of gas-filled cavity . . . . .	22
3.5	Abaqus . . . . .	23
3.6	Calfem . . . . .	24
<b>4</b>	<b>IGU finite element modeling</b>	<b>25</b>
4.1	Material and geometry . . . . .	25
4.2	Elements and mesh . . . . .	26
4.3	Loads and boundary conditions . . . . .	26
4.4	Solution procedure . . . . .	26
4.4.1	Instability problem . . . . .	29
4.5	Implementation in Matlab . . . . .	29
4.6	IGU finite element modeling in Abaqus . . . . .	29
4.6.1	Purpose . . . . .	29
4.6.2	Geometry and material . . . . .	30
4.6.2.1	Elements and mesh . . . . .	30
4.6.3	Loads and boundary conditions . . . . .	31
<b>5</b>	<b>Numerical studies</b>	<b>33</b>
5.1	Evaluation of the developed method . . . . .	33
5.1.1	Temperature change . . . . .	33
5.1.2	Pressure change . . . . .	36
5.1.3	Wind load . . . . .	36
5.1.4	Three glass IGUs . . . . .	37
5.1.5	Non-linear geometry . . . . .	37
5.1.6	Discussion of evaluation . . . . .	38
5.2	Comparison with experimental data . . . . .	38
5.2.1	Discussion of comparison analysis . . . . .	41
<b>6</b>	<b>Discussion and further work</b>	<b>43</b>
6.1	Discussion . . . . .	43
6.2	Conclusion . . . . .	44
6.3	Further work . . . . .	44
<b>A</b>	<b>Matlab code</b>	<b>47</b>
A.1	Main program . . . . .	47

# Chapter 1

## Introduction

### 1.1 Background

Glass is a popular facade material in buildings since it gives an attractive design and let natural light into the building. But the insulating capacity of single glass pane do not satisfy the rapidly increasing request for energy efficiency. Insulating glass units is a good solution for increasing the insulating capacity as well as keeping the desirable design of glass.

Insulating glass units (IGUs) normally consists of two or three glass panes which encase a hermetically sealed cavity filled with gas. The gas in the cavity is usually argon gas but also air and krypton is used as a filler gas.

Since the cavity is hermetically sealed the gas content will not change and the gas pressure will depend on the volume of the cavity dimensions, the ambient pressure and the temperature of the gas. If the temperature or the pressure differs from the initial values the gas will try to expand or compress and a deformation (bulging) of the glass panes will develop without any other external loads applied to the structure.

This phenomenon may worsen if the change in temperature and pressure combine in a negative fashion. For example on a cold day with a low atmospheric pressure, the loads both will create an inward bulging and increase the stress in the glass. This scenario can be aggravated if an external load is applied to the window, such as wind load. The natural change in weather will thus affect the IG unit substantially. The development of bulging will lead to tensile stresses in the glass which is a problem if the glass has a low tensile strength. If the tensile stress exceeds the tensile strength the glass will fracture. For windows with small dimensions the tensile stresses will be the main problem whereas large deformations will be the main problem for IG units with large dimensions.

### 1.2 Objective, aim and method

The objective of this thesis is to create a computational method with the ability to calculate the deformation and the stress in an IGU. The method must be able to handle various dimensions of the IGU and different load types, such as temperature change, change in ambient pressure and wind load. The developed method can handle IGU with

two or three glass panes.

The aim of the developed method is that it can be implemented in ClearSight, a glass design program that is used by the Swedish glass building industry.

The computational method will use the finite element method to solve the problem. The FE-analysis will be created using Calfem within Matlab which is a FE toolbox with the essential functions to create a FE-analysis. The finite element method is an effective way of calculating advanced physical problems. Later on, the method should be able to be implemented in a more effective programming language such as Fortran.

The computational method is verified using the finite element program Abaqus. Similar models are created in Abaqus and Calfem and the two models are compared with various choice of parameters such as load and dimensions. The computational method is also compared with the result of a master thesis made by Martin Andersson and Simon Nilsson, [11]. They made FE-analyzes and experimental tests of IGUs exposed to temperature changes.

### 1.3 Limitation

The developed method will only handle rectangular shapes of the IGU. More advanced geometries requires a more advanced model and the model has to be adjusted for every change in the geometry. With rectangular shapes the model is easy to change by scaling the length and height of the dimensions. Usually the IGUs are manufactured with rectangular geometry, so the need for different geometries is not a priority.

There is no automated way to model more than two cavities and three glass panes in the method. It is however, straight forward to adapt the model to several layers.

The developed method can only handle linear geometry. Simulations in Abaqus regarding non-linear geometry was made to evaluate the impact of non-linear geometry on the deformations.

The glass panes are modeled with the properties of float glass but any properties may be given to the glass panes.

### 1.4 Outline

- Chapter 2: A description of the structure, manufacturing of IGUs and a summary of earlier studies is given.
- Chapter 3: The theory used to create the method is explained. This chapter contains the theory behind the physical phenomenon of the gas, the theory of the finite element method, the load cases that the IGU can be exposed to and the interaction between the gas and the structure is explained.
- Chapter 4: The content consists of a description of how the method was modeled with FEM and implemented in Matlab and a description of how an IGU was modeled using Abaqus. A summary of parameters and boundary conditions that were used in the analyzes.

- Chapter 5: Numerical studies to evaluate the computational method is presented.
- Chapter 6: A discussion of the method and the result is presented. A conclusion of the work and suggestions of further work are given.



# Chapter 2

## Insulating glass unit

### 2.1 Earlier studies

In [11] FE-analyzes and experimental tests of IGUs were represented. The experimental tests were carried out on five different IGUs, the dimensions of the units are presented in Table 2.1. The IG units were manufactured at the temperature of 20° C and an atmospheric pressure during manufacturing of 100.9 kPa.

Table 2.1: Dimensions of IGUs used in experimental test [11].

IGU	Dimensions [mm]		Glass thickness [mm]			Cavity depth [mm]	
	Width	Height	Outer	Middle	Inner	Outer	Inner
1	1200	1200	6	4	4	22	16
2	1200	1200	4	4	4	24	24
3	1200	1200	4	4	4	22	16
4	600	600	4	4	4	24	24
5	1800	1200	4	4	4	22	16

The material data that was used for the glass in [11] are presented in Table 2.2.

Table 2.2: Material properties used by [11].

Young's modulus	70 GPa
Poisson's ratio	0.22
Density	2500 kg/m <sup>3</sup>

In [11] the stiffness of the spacer was presented. Experimental data and Hooke's law was used to establish an expression for the Young's modulus which is shown in Equation (2.1).  $h_{spacer}$  in the equation was set to either the height or width of the IGU depending on where the spacer was located. The Poisson ratio of the spacer was assumed to be 0.3 and the thickness of the spacer was 6 mm.

$$E_{spacer} = 2.9 \cdot h_{spacer} GPa \quad (2.1)$$

The Young's modulus of butyl and polysulfide, which are used as sealants in IGUs, varies with change in temperature [20]. But the difference between the Young's modulus is small and was neglected [11]. The Young's modulus of the sealant was set to 1.6 MPa and the Poisson ratio of the sealant was assumed to be 0.2. The thickness of the sealant was set to 6 mm.

In [11] three different experimental tests were performed. In Test 1 the deformations of IGUs exposed to different temperatures on each side was measured. The experimental conditions of this test is presented in Table 2.3.

Table 2.3: Conditions for the IGUs during Test 1 [11].

IGU	Cold glass surface [°C]	Middle glass [°C]	Warm glass surface [°C]	Atmospheric pressure [kPa]
1	-11.6	1.6	13.7	101.7
2	-12.1	3.7	14.6	101.4
3	-11.9	1.9	14.3	101.2
5	-9.2	2.6	19.3	101.3

The result of Test 1 is shown in Table 2.4 which shows the results from the FE-analyzes and Table 2.5 which shows the results from the experimental tests [11].

Table 2.4: Displacement of glass and the total bulging in the center of the glass pane from FE-analyzes in Abaqus of Test 1, [11]

IGU	Displacement			Total bulging in middle [mm]
	Outer	Middle	Inner	
1	2.32	-2.25	-3.92	6.24
2	3.82	-0.92	-3.18	7.00
3	3.35	-1.02	-2.57	5.92
4	-	-	-	-
5	3.64	-1.09	-2.80	6.44

Table 2.5: Displacement of glass and the total bulging in the center of the glass pane from experimental tests of Test 1, [11]

IGU	Abaqus		
	Displacement [mm]		Total bulging in middle [mm]
	Outer	Inner	
1	3.1	5.7	8.8
2	6.3	4.5	10.8
3	6.0	5.1	11.1
4	-	-	-
5	6.7	3.4	10.2

In Test 2 the IGUs were exposed to  $-10.15^{\circ}\text{C}$  on both sides and the atmospheric pressure during the test was 101.6 kPa [11].

The result of Test 2 is shown in Table 2.6 which shows the results from the FE-analyzes and Table 2.7 which shows the results from the experimental tests [11].

Table 2.6: Displacement of glass and the total bulging in the center of the glass pane from FE-analyzes in Abaqus of Test 2, [11]

IGU	Displacement			Total bulging in middle [mm]
	Outer	Middle	Inner	
1	-	-	-	-
2	5.70	0	-5.7	11.41
3	4.77	-0.60	-4.49	9.26
4	4.08	0	-4.08	8.15
5	4.83	-0.59	-4.51	9.34

Table 2.7: Displacement of glass and the total bulging in the center of the glass pane from experimental tests of Test 2, [11]

IGU	Abaqus		
	Displacement [mm]		Total bulging in middle [mm]
	Outer	Inner	
1	-	-	-
2	8.1	7.0	15.1
3	6.8	6.3	13.1
4	5.9	5.7	11.5
5	7.0	5.8	12.8

In the last test, Test 3, the IGUs were placed in the laboratory hall [11]. The IGUs were covered with opaque plastic to prevent increase of temperature due to radiation. The temperature during Test 3 was  $20.9^{\circ}\text{C}$  and the atmospheric pressure was 102.2 kPa.

Test 3 was used to establish the residual deformations which were obtained in the laboratory analysis [11].

The result of Test 3 is shown in Table 2.8 which shows the results from the FE-analyzes and Table 2.9 which shows the results from the experimental tests [11].

Table 2.8: Displacement of glass and the total bulging in the center of the glass pane from FE-analyzes in Abaqus of Test 3, [11]

IGU	Displacement			Total bulging in middle [mm]
	Outer	Middle	Inner	
1	0.26	-0.22	-0.57	0.83
2	0.53	0	-0.53	1.06
3	0.44	-0.04	-0.40	0.84
4	0.38	0	-0.38	0.77
5	0.44	-0.05	-0.40	0.84

Table 2.9: Displacement of glass and the total bulging in the center of the glass pane from experimental tests of Test 3, [11]

IGU	Abaqus		
	Displacement [mm]		Total bulging in middle [mm]
	Outer	Inner	
1	1.4	2.9	4.3
2	3.5	2.2	5.7
3	4.3	2.5	6.8
4	1.6	1.6	3.2
5	3.1	1.5	4.6

During the experimental analysis the total bulging were measured, meaning the combined displacement of the two outer glass panes. This is illustrated in Figure 2.1 where  $\delta_1$  and  $\delta_2$  is the deformation of the two outer glass pane and the total bulging is equal to  $\delta_{tot} = \delta_1 + \delta_2$

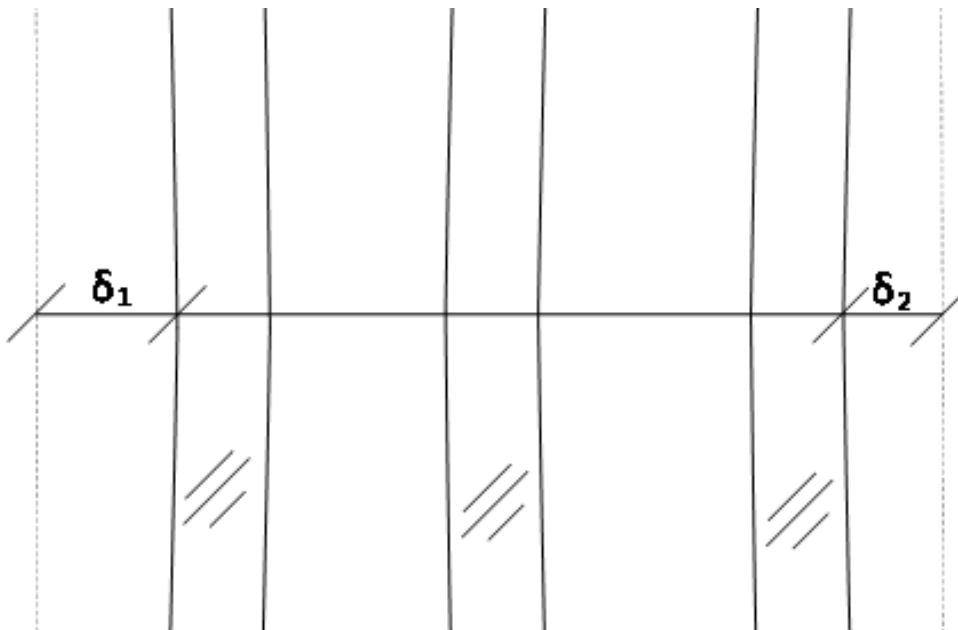


Figure 2.1: Illustration of total bulging [11].

In [16] a formulation of a two-dimensional ideal gas finite element which could be used in studies of IGUs is presented. According to the authors this finite element can be expanded to a three-dimensional element.

Modeling of IGUs in Abaqus a hydrostatic fluid element is used which is described in [23]. A single volume element is used to represent the gas volume. This is defined by the bounding surface of the cavity which is similar to the implementation of the computational method in this thesis. In [24] a simple method for FE-analysis of IGUs is presented where Kirchhoff's plate theory is used for establishing the FE-analysis.

## 2.2 IGU structure

Insulating glass units consists normally of two or three glass panes divided by a spacer. The spacer is filled with a desiccant to prevent moisture within the cavity. The cavity is filled with a gas, usually argon, to increase the insulating capacity of the unit. To prevent leakage in the cavity a sealant is placed between the spacer and the glass panes. This is called the primary sealant and has a low permeability. To protect the primary sealant, a secondary sealant is placed around the spacer between the glass panes. Various types of glass can be used in IGUs, for example, low-E glass can be used for better insulating capacity or toughened and laminated glass for increased strength.

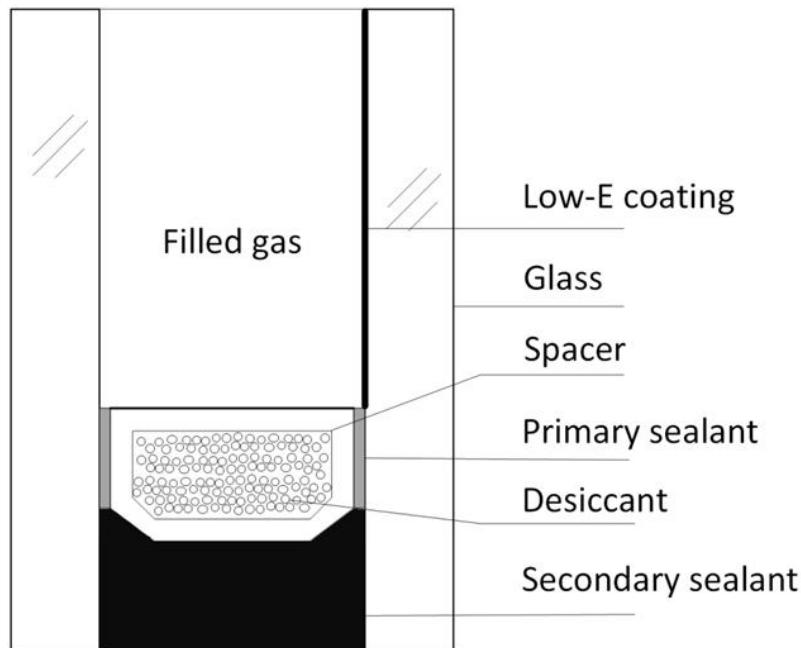


Figure 2.2: Basic structure of doubled sealed insulating glass unit [11].

### 2.2.1 Glass

Glass is a solid material with amorphous structure, meaning that the atomic pattern is irregular, similar to a sub cooled liquid, which makes it transparent [2]. The structure of glass makes it a brittle material which means that fractures arise without any plastic deformation.

The most common method for manufacturing glass for constructional use is the float glass process [1]. When the glass is manufactured different modifications can be made to change its attributes. Modifications such as lamination and toughening can be used to increase the strength and by applying coatings to the glass the insulating capacity can be increased.

To create glass the material used has to be an oxide which during cooling does not crystallize but transcend into an amorphous condition [1]. The most used material is silicone dioxide (quartz) which is obtained in sand. The purity of the sand is therefore important to create high quality glass. To lower the melting point of the quartz a flux material is added. The flux material is an oxide, for example sodium oxide. The combination of the oxides has low chemical and moisture resistance so a stabilization material is added.

### 2.2.1.1 Float glass

The float glass process was developed by Pilkington in 1959 [1]. The process starts by mixing and crushing the exact proportions of the raw materials needed, this mixture is called soda-lime-silica glass [5]. The crushed material can be mixed with recycled glass before it is fed into a furnace and melted. The molten glass is then constantly fed on to the surface of a float bath that consist of molten tin. The surface of the tin bath is almost perfectly plane which makes the glass even [2]. If the glass may float freely the thickness becomes 7 mm and by either pulling or pressing the glass the thickness can be regulated between 0.4 and 25 mm [2]. The glass is then cooled at a slow rate to room temperature, this is called annealing and glass created by this process is called annealed glass. When the temperature of the glass has reached the room temperature the glass is cut to the wanted dimension [1]. Glass, especially the surface, consist of a large unknown number of micro-cracks which may lead to fracture [3]. The number of micro-cracks and the indication of fracture from the cracks varies from each specimen of glass. Also the quality of the cut affects the strength of the glass [3]. When annealed glass breaks it turns into sharp shards which can lead to injuries. Figure 2.3 shows an illustration of the float process.

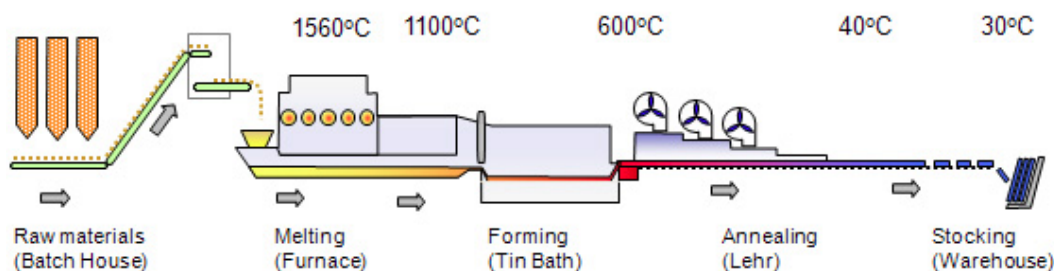


Figure 2.3: The float process [14].

### 2.2.1.2 Types of glass

Annealed glass is the primary component used to create customized glass products, such as toughened glass and low-E glass. These are used for circumstances when normal glass does not fulfill the requirements.

To reduce the effects of micro-cracks that develops in the glass, the surface should be exposed to compressive stress. This can be obtained by toughening the glass and the most common process is thermal toughening [2]. The glass pane is heated to 600 °C and then cooled rapidly [3]. When the temperature decrease rapidly the glass surface will cool of faster than the middle of the glass pane. This creates compressive stress in the surface and tensile stress in the center of the pane. Thermal toughening increase the compressive and tensile strength by 4-5 times but the stiffness of the glass is still the same, meaning that the deformation will be the same as for normal glass during loading [3]. After thermal toughening no changes can be made to the glass, so cutting and processing has to be done before the glass is exposed to toughening. When toughened glass breaks it shatters as annealed glass but the shards is not as sharp, this makes toughened glass suitable as security glass [2].

Laminated glass is created by placing a plastic film between two or more glass panes and press the glass panes together during heating [3]. An illustration of laminated glass is shown in Figure 2.4. When fracture occurs the plastic film holds the glass shards in place. This will keep the glass pane in the outside construction. The strength of the glass can be a bit lower and the deformation a bit higher than normal glass of the same total thickness. But when laminated glass breaks the fragments of glass shards will be retained in the glass pane and the risk of injury by cuts from the shards is lower. Laminated glass is used as security glass. The glass panes in the laminated glass can be annealed glass or heat treated glass or a combination both [7]. The plastic film is normally PVB (polyvinyl butyral) but can differ [2].

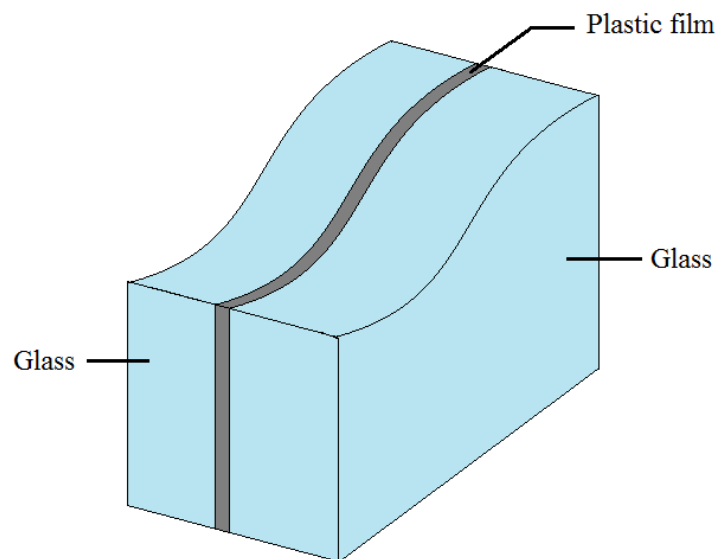


Figure 2.4: Structure of laminated glass.

### 2.2.1.3 Mechanical properties of glass

Glass is an ideal elastic material which means that it deforms elastically during stress and no plastic deformations appear before fracture [1]. The fact that no plastic deformation appears makes glass sensitive to point loads, since plastic deformation can redistribute the load, as seen in steel [7]. The strength of the glass is also dependent on the duration of the load [3]. The theoretical tensile strength is based on the molecular forces within the

glass and is very high. However, the actual tensile strength, which is used for structural application, is much lower than the theoretical strength [7]. The reason for the difference between theoretical strength and the actual strength depends on flaws on the surface, micro-cracks [7]. Flaws, such as micro-cracks, are usually not visible to the eye so the glass has to undergo quality control during manufacturing [2].

Fracture occurs in glass when the stress intensity due to tensile stress reach the critical value of one micro-crack [7]. The flaws increase over time if the element is loaded, which indicate that glass is sensitive to long duration load. Micro-cracks does not fail under compression, so the compressive strength of glass is much higher than the tensile strength. This is irrelevant for most glass structures since tensile stress develop during bulging and therefore will the loaded element exceed the tensile strength before the compressive strength is exceeded.

In most of the simulations in this report the properties of the glass had was chosen according to Table 2.10

Table 2.10: Mechanical properties for glass.

Young's modulus	73 GPa
Poisson's ratio	0.22
Density	2500 kg/m <sup>3</sup>

## 2.2.2 Spacer and sealants

To create and retain a cavity between the glass panes and keep the gas in the cavity a spacer is mounted between the glass panes [4]. The spacer can be made of stainless steel, aluminium or a plastic spacer covered with steel foil.

In most cases a plastic spacer covered with steel is used [4]. A plastic spacer has lower heat conductivity than both aluminium and stainless steel but plastic is not gas-impermeable. Therefore when using a plastic spacer the spacer is usually coated with an aluminium or stainless steel foil.

Within the spacer a desiccant is placed to absorb the moisture within the cavity.

The main function of the sealant is to structurally hold the spacer and the glass panes together while also prevent leakage of gas and moisture to the cavity [5]. There are two methods used for sealing insulating glass units, single- or doubled-sealed method, illustrated in Figure 2.5. When looking at life expectancy of an insulating glass unit the doubled sealed method is usually the best choice [6].

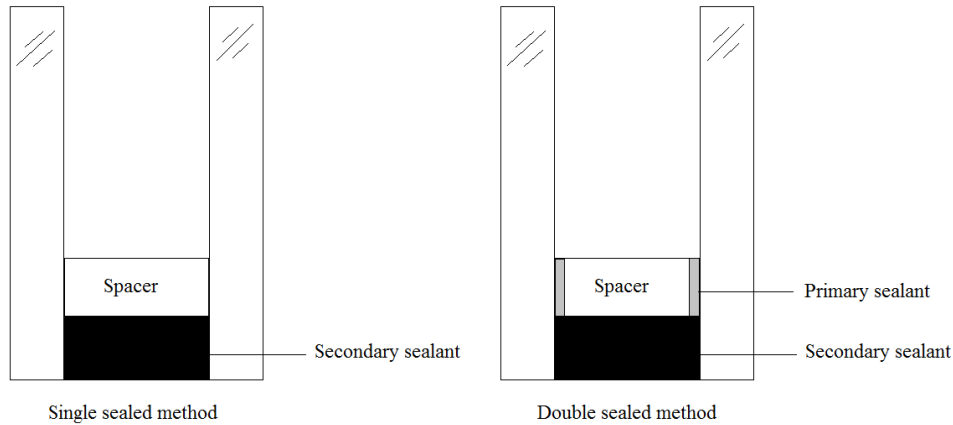


Figure 2.5: Illustration of single- and double-sealed method.

In the double-sealed method, two types of sealants are used [6]. One sealant is placed between the spacer and the glass panes. This sealant is called the primary sealant and will prevent moisture and gas leakage. The other sealant is placed around the spacer and between the glass panes and will bond the glass panes together, protect the primary sealant and reduce the permeability of gas and moisture.

In a single-sealed system one sealant is used and is placed as the secondary sealant in a double-sealed system [6]. The sealant in a single-sealed system has to compensate for the lack of a primary sealant. Therefore, in a single-sealed system, the sealant should be impermeable.

### 2.2.2.1 Primary sealant

Polyisobutene also known as butyl is the most common material for the primary sealant [6]. Butyl has good properties for preventing moisture from forming within the cavity as well as preventing gas to escape the cavity. Butyl has also an adhesive effect between the spacer and the glass panes [4]. Butyl is thermoplastic, meaning that it will lose strength when the temperature increases [6]. Therefore will butyl not be enough to guarantee structural functionality of the unit and the use of a secondary sealant is inevitable.

### 2.2.2.2 Secondary sealant

The secondary sealant works as a bond between the spacer and the glass panes and also as a vapor protection toward the primary sealant [5]. The material selected for the secondary sealant depends on the circumstances. One of the most common type is polysulfide which has good adhesion to glass and low permeability of gas. Polysulfide is sensitive to short wavelength radiation such as ultraviolet radiation from the sun and it swells when it absorbs water. Therefore, polysulfide, must be protected from direct sun light and humid conditions. Polyurethane is another common sealant [5]. The permeability of polyurethane is low for water vapor and is flexible at low temperature [6]. The mechanical properties for polyurethane is also good. The disadvantages of polyurethane is that the permeability of the gas is fairly high in comparison with polysulfide and the sealant will swell when absorbing water [6]. As for the case with polysulfide, polyurethane is sensitive

to short wave radiation. Both polysulfide and polyurethane is only used in double-sealed systems [5]. One product group which is used in both double- and single- sealed system is silicone. When absorbing water the swelling is small compared to other sealants and it has good resistance towards short wave radiation [6]. One of the disadvantages of silicone is the permeability of the gas is fairly high and measures has to be made with regards to this during manufacturing of insulating glass units with silicone sealants [6].

## 2.3 Cavity

The cavity between the glass panes is filled with air and usually some noble gas. Argon and krypton is common as filler gases because they have lower heat conductivity and have higher dynamic viscosity than air. When using these gases within the cavity both the heat conductivity and the convection is lowered for the insulating glass unit [3]. Krypton has better insulating capacity than argon and only need 10-12 mm interspace between the glass panes for optimal insulating efficiency while argon needs an interspace of 15-18 mm for the same effect [4]. Krypton is more expensive and that is why argon is the most used filler gas in insulating glass units. The cavity is usually filled with an mix of 90 % of noble gas and 10 % of air [4].

# Chapter 3

## Theory

### 3.1 Ideal gas in enclosed cavity

IGUs will be exposed to temperature variation, volume change and change in atmospheric pressure. These three parameters will affect the gas in the cavity in different ways. The relationship between these quantities is expressed with the ideal gas law (3.1) [12].

$$pV = nRT \quad (3.1)$$

where  $p$  is the gas pressure,  $V$  is the volume of the gas,  $n$  is the amount of substance in the gas,  $R$  is the gas constant which is equal to  $R = 8.314 \text{ [J/(molK)]}$  and  $T$  is the temperature in the gas.

Since the cavity is hermetically sealed, the amount of substance is constant during the analysis of an IGU. This means that the gas that is used as a filler gas is not essential for the analysis.

$$nR = \text{constant} \quad (3.2)$$

For an isothermal process, when the temperature is constant, the ideal gas law can be expressed with Eq. (3.3), [12]. During an isothermal process all the energy in the gas will be transferred to mechanical energy.

$$pV = \text{constant} \quad (3.3)$$

Since the gas in the cavity is a closed system, the volume change will lead to a change in gas pressure. A volume change of the cavity originates from the deformation of the glass panes, which will develop during loading.

Change in ambient pressure will lead to a change in gas pressure that in turn will induce a volume change of the cavity. A high- or low-pressure in the atmosphere will act as a change in ambient pressure. The atmospheric pressure also depends on the geographic locations where the insulating glass unit was manufactured and installed. The average difference of the atmospheric pressure is 0.5 kPa higher in the southern part of Sweden as compared to the northern part, but the difference can be higher between specific locations [8].

A temperature change in the cavities will change both the volume and the pressure of the gas. A temperature lower than the initial temperature will, for constant ambient pressure, lead to inward bulging and a higher temperature will lead to an outward bulging.

Any change from the initial temperature and pressure will lead to a volume change, i.e. bulging of the glass pane.

### 3.1.1 Initial conditions for the gas

The temperature change and pressure change depends on the conditions of the gas when the IGU was assembled. This will vary depending on the location where and when the unit was manufactured. For the simulations made in this report the IGU was assumed to be manufactured inside a factory and under normal atmospheric pressure. The initial conditions for the gas which were used for simulations later on in this report is shown in Table 3.1. The atmospheric pressure is a standard value used in Sweden[8, 12].

Table 3.1: Assumed initial conditions for the gas.

Atmospheric pressure	101.325 kPa
Temperature	20°C

## 3.2 Load cases

The IGU is sensitive to climate load such as change in atmospheric pressure and temperature change. This change depends on the location of the manufacturing factory and the location where the IGU is installed. Since the IGU will be placed in the facade of the building it will be exposed to wind load as well.

The climate conditions are assumed to be known when the IGU is assembled. At this stage it is also assumed that there is no bulging in the glass pane. The pressure of the gas is known from the atmospheric pressure and the temperature is also known at the time of assembly. The initial conditions of the analysis might differ from the conditions at assembly and should then be considered as loads. The conditions of the gas can be divided into three stages, the conditions at assembly, the conditions when the analyze start and the current condition. In the analyzes in this thesis the initial conditions of the gas is assumed being identical to when the IGU was assembled.

If the atmospheric pressure change, either from location difference or climate change, an increase or decrease in pressure will occur in the cavity.

The temperature difference will create a change in pressure and volume. The change in pressure from a change in temperature can be expressed from the ideal gas law as

$$\Delta p = nR(T + \Delta T)/V_0 - p_0 \quad (3.4)$$

where  $V_0$  is the initial volume.

When the IGU is exposed to wind load the outer glass pane will deform which will reduce the volume of the gas. The pressure will reduce the deformation of the outward

glass pane but will induce a deformation on the inward glass pane, as illustrated in Figure 3.1. A common wind load is approximately around 1 kPa in Sweden but can be larger depending on the specific circumstances where the load is calculated [13]. This is relatively small compared to the load induced by temperature variation and change in atmospheric pressure. But since a the gas pressure effects all the glass panes in the IGU, when it is subjected to wind load, is it still interesting to calculate the effect of this load. The wind load depends on the height from the ground, the geographic location and the surrounding terrain. The dimensioning wind load can be obtained for different locations using Eurocode.

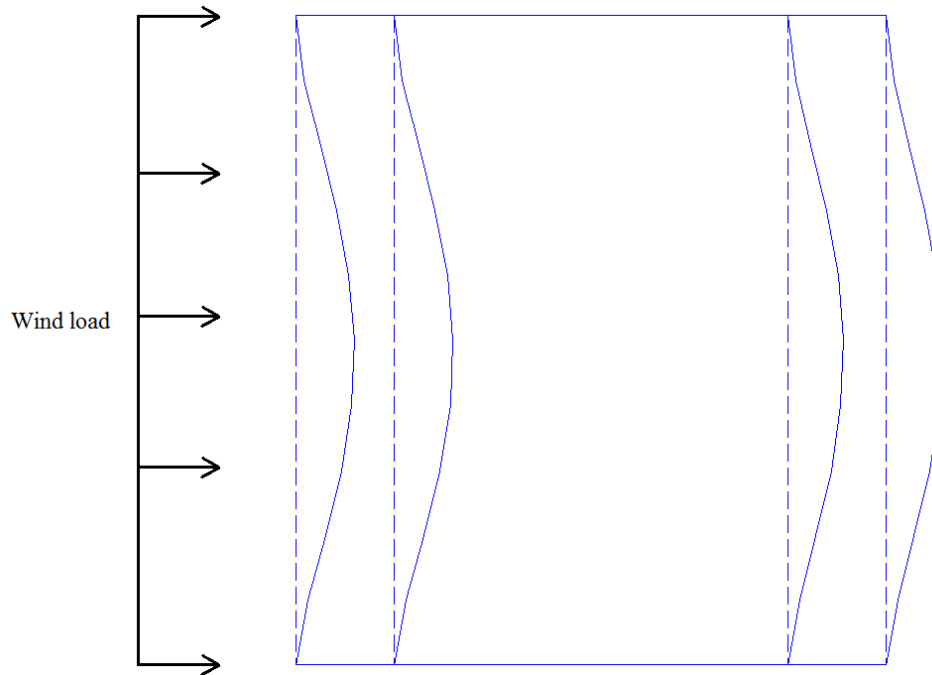


Figure 3.1: Illustration of deformation induced by wind load on a IGU with one cavity.

The IGU can also be exposed to other loads such as accidental loads, for example a bird crashing into the window. This load case is not further investigated in this thesis.

## 3.3 Finite element method

### 3.3.1 General

Physical problems which occurs in structural mechanics can most often be described by partial differential equations [9]. For simple cases the differential equations can be solved by analytical methods but these are insufficient if the boundary conditions or the geometry becomes complex. To solve these problems, the finite element method can be used that finds approximate solution to the differential equations by numerical calculations.

In the FE-method the structure is divided into smaller parts, so called finite elements [9]. The FE-method is used to find approximate solutions for each element which then can be assembled to find an approximate solution for the entire structure. The collection of

all the elements is called a finite element mesh. The more elements used the better the approximation becomes but the more elements used the longer the calculation time and computer capacity is needed. So a consideration has to be made of how many elements is needed in order to obtain a decent solution which can be carried out in a reasonable time and with the computer capacity at hand. The FE-method can be applied to various physical problems since it is a numerical solution to general differential equations. The method can be used for structures which are defined in one, two or three dimensions.

The FE-method gives an interpolated approximation of how a variable change over each element [9]. The method assume that the variable is known in certain points, nodal points, of the element, usually located in the boundary of each element. Each nodal point, or node, consist of a number of unknown variables, the amount of unknown in a node is called degree of freedom or DOF. To determine the values of the unknown variables a certain system of equations has to be solved. For a large FE-system, thousands of equation has to be solved which is impossible to do by hand and that is the reason why the calculations is carried out with a computer.

The sum of all forces acting on the element is equal to zero, this can be expressed with the equilibrium equation

$$\mathbf{K}\mathbf{a} = \mathbf{f}_b + \mathbf{f}_l \quad (3.5)$$

where

$$\mathbf{K} = \int_V \mathbf{B}^T \mathbf{D} \mathbf{B} dV, \quad \mathbf{f}_b = \int_S \mathbf{N}^T \mathbf{t} dS, \quad \mathbf{f}_l = \int_V \mathbf{N}^T \mathbf{b} dV \quad (3.6)$$

$\mathbf{K}$  is the stiffness matrix,  $\mathbf{a}$  is the nodal displacement vector,  $\mathbf{f}_b$  is the boundary vector and  $\mathbf{f}_l$  is the load vector.

### 3.3.2 Elements

The elements used in the FE-calculations were modeled with M-RESS 3-D solid-shell elements with eight nodes. Each element consist of 24 DOF, three in each node which represents  $x$ -,  $y$ - and  $z$ -direction. The deformation was assumed to vary linear over the element. An illustration of the element used in the Calfem calculations is illustrated in Figure 3.2.

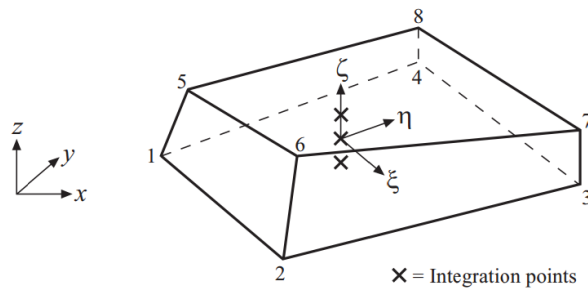


Figure 3.2: 3-D element used in Calfem model [21].

In Figure 3.2 one can see that there are two coordinate systems shown in the figure. The reason for this is that the element is isoparametric and not restricted by a criteria that the sides of the element has to be parallel to the coordinate axes to behave in a compatible manner [9].

M-RESS Solid-shell elements are 3-D hexahedral solid elements [21]. M-RESS is short for Modified Reduced in-plane integration, Enhanced strain field, Solid-Shell element. The advantages of using M-RESS elements is the increase in computational efficiency since the element use a reduced integration scheme with several integration points only in the local axis along the thickness direction,  $\zeta$  in Figure 3.2.

### 3.3.3 Linear elasticity

Linear elasticity means that the stress is proportional to the strains in a material. For small deformation and in one dimension the linear elasticity can be expressed by Hooke's law,

$$\sigma = E\epsilon \quad (3.7)$$

where  $E$  in Hooke's law is a material constant which is called Young's modulus and is a measurement of stiffness in an elastic material.

This expression can be expanded for two and three dimensions and then it is referred to as Hooke's generalized law [9]. The stresses and strains are then given in several components and can be written as

$$\boldsymbol{\sigma} = \mathbf{D}\boldsymbol{\epsilon} \quad (3.8)$$

where

$$\boldsymbol{\sigma} = \begin{bmatrix} \sigma_{xx} \\ \sigma_{yy} \\ \sigma_{zz} \\ \sigma_{xy} \\ \sigma_{xz} \\ \sigma_{yz} \end{bmatrix}; \quad \mathbf{D} = \begin{bmatrix} D_{11} & D_{12} & \dots & D_{16} \\ D_{21} & D_{22} & \dots & D_{26} \\ \vdots & \vdots & \ddots & \vdots \\ D_{61} & D_{62} & \dots & D_{66} \end{bmatrix}; \quad \boldsymbol{\epsilon} = \begin{bmatrix} \epsilon_{xx} \\ \epsilon_{yy} \\ \epsilon_{zz} \\ \epsilon_{xy} \\ \epsilon_{xz} \\ \epsilon_{yz} \end{bmatrix} \quad (3.9)$$

and  $\mathbf{D}$  is a constitutive matrix. The  $\mathbf{D}$ -matrix is by the looks of it a 6x6-matrix with 36 independent coefficients but due to symmetry it only consist of 21 independent coefficients [10]. For an isotropic material there will be three symmetry planes which will reduce the constitutive matrix further.

To develop the matrix further the Poisson's ratio  $\nu$  is introduced, which is the ratio between what strain in one direction is caused by a loading in another direction [10]. For the relation between shear stress and shear strain the shear modulus  $G = \frac{E}{2(1+\nu)}$  is introduced. With these parameters Hooke's generalized law may be written as

$$\begin{bmatrix} \epsilon_{xx} \\ \epsilon_{yy} \\ \epsilon_{zz} \\ \epsilon_{xy} \\ \epsilon_{xz} \\ \epsilon_{yz} \end{bmatrix} = \begin{bmatrix} \frac{1}{E_1} & -\frac{\nu_{21}}{E_2} & -\frac{\nu_{31}}{E_3} & 0 & 0 & 0 \\ -\frac{\nu_{12}}{E_1} & \frac{1}{E_2} & -\frac{\nu_{32}}{E_3} & 0 & 0 & 0 \\ -\frac{\nu_{13}}{E_1} & -\frac{\nu_{23}}{E_2} & \frac{1}{E_3} & 0 & 0 & 0 \\ 0 & 0 & 0 & \frac{1}{G_{12}} & 0 & 0 \\ 0 & 0 & 0 & 0 & \frac{1}{G_{13}} & 0 \\ 0 & 0 & 0 & 0 & 0 & \frac{1}{G_{23}} \end{bmatrix} \begin{bmatrix} \sigma_{xx} \\ \sigma_{yy} \\ \sigma_{zz} \\ \sigma_{xy} \\ \sigma_{xz} \\ \sigma_{yz} \end{bmatrix} \quad (3.10)$$

For a homogenous isotropic material the constitutive matrix does not depend on position no matter what coordinate system used [10]. With this in mind, for an isotropic linear elastic material the constitutive matrix can be written as

$$\mathbf{D} = \frac{E}{(1+v)(1-2v)} \begin{bmatrix} 1-v & v & v & 0 & 0 & 0 \\ v & 1-v & v & 0 & 0 & 0 \\ v & v & 1-v & 0 & 0 & 0 \\ 0 & 0 & 0 & \frac{1}{2}(1-2v) & 0 & 0 \\ 0 & 0 & 0 & 0 & \frac{1}{2}(1-2v) & 0 \\ 0 & 0 & 0 & 0 & 0 & \frac{1}{2}(1-2v) \end{bmatrix} \quad (3.11)$$

In Equation (3.11) the constitutive matrix is now expressed with two independent coefficients, Young's modulus  $E$  and Poisson's ratio  $v$ , which are known material parameters. The D-matrix was used to calculate the element stiffness matrix in the finite element calculations.

### 3.3.4 Element load

The element load vector for each 3-D element was calculated as an equivalent node load in the same manner as for a 2-D plane element. Equation (3.12) defines the element load vector with the size [4x1].

$$\mathbf{f}_i^e = \int_A \mathbf{N}^{eT} q t dA \quad (3.12)$$

Where  $\mathbf{N}$  is the element shape function,  $q = q(x, y)$  is the amplitude of the force acting on the element,  $t$  is the thickness and  $A$  is the surface area of the 3-D element. The shape function is given by the x- and y-coordinates of the element.

The element force vector gives an equivalent load in each node which the force act on. These are then assembled in the global force vector.

## 3.4 Interaction between gas and structure

### 3.4.1 Volume change

The FE-model contain the glass and the spacer, this means that the gas in the cavity was not modeled by finite elements. Instead, the volume change is calculated and from that the pressure is applied as a load. The volume of the gas was calculated with the coordinates of the elements facing the cavity and a reference node inside the cavity. The gas pressure was applied as a uniformly distributed load acting orthogonal towards the surface.

A reference node was created within the cavity. The node can be placed anywhere but out of convenience it was placed in the middle of the cavity. With this node and the nodes that defines the finite elements on the surface of the cavity, volume elements can be created. One volume element is defined by five nodes, four nodes at the element on the surface and the reference node within the cavity. These five nodes created a pyramid shaped element from which the volume could be calculated, see Figure 3.3. The total volume of the cavity is the sum of all volume elements.

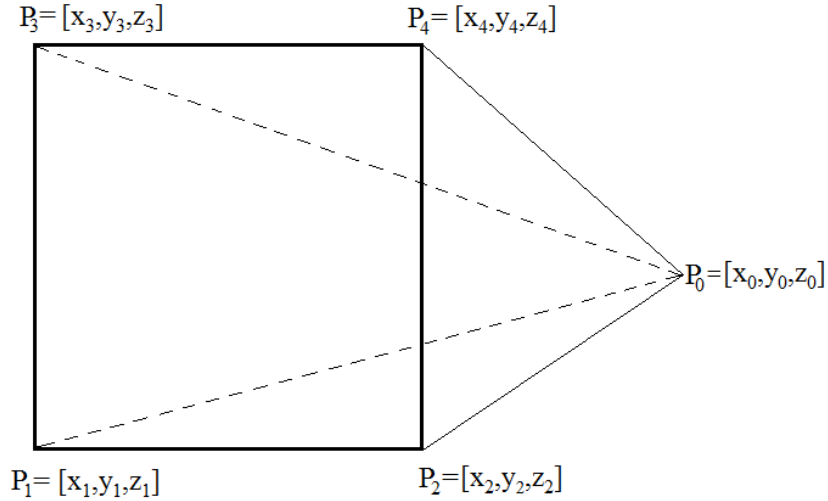


Figure 3.3: Pyramid of which the volume can be calculated.

The pyramid that was defined by the nodes can be divided into two tetrahedrons for easier calculations. The volume of the pyramid is the sum of the two tetrahedron volumes.

A tetrahedron with four nodes, see Figure 3.4

$$P_1 = [x_1, y_1, z_1], P_2 = [x_2, y_2, z_2], P_3 = [x_3, y_3, z_3], P_0 = [x_0, y_0, z_0]$$

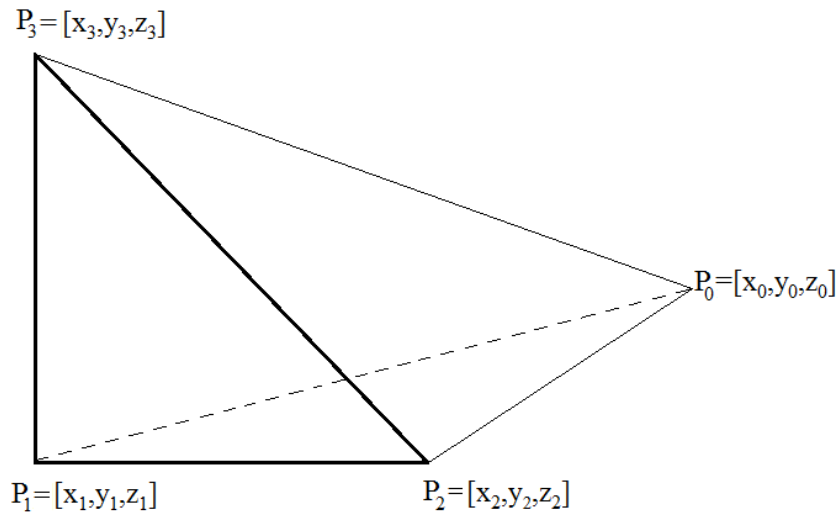


Figure 3.4: Definition of the nodes that creates a tetrahedron for volume calculations.

The volume of a tetrahedron which is defined by these points are obtained by

$$V_{tetrahedron} = \frac{1}{6} \det \begin{bmatrix} x_1 - x_0 & x_2 - x_0 & x_3 - x_0 \\ y_1 - y_0 & y_2 - y_0 & y_3 - y_0 \\ z_1 - z_0 & z_2 - z_0 & z_3 - z_0 \end{bmatrix} \quad (3.13)$$

With Eq. (3.13), the volume for a volume element in the cavity could be obtained by use of Eq. (3.14). The nodes which defines the pyramid shaped element can be written as

$$P_1 = [x_1, y_1, z_1], P_2 = [x_2, y_2, z_2], P_3 = [x_3, y_3, z_3], P_4 = [x_4, y_4, z_4], P_0 = [x_0, y_0, z_0]$$

where  $P_1, P_2, P_3$  and  $P_4$  are the nodes on the surface and  $P_0$  is the reference node in the cavity, as shown in Figure 3.3.

$$V_{elvol} = \frac{1}{6} \det \begin{bmatrix} x_1 - x_0 & x_2 - x_0 & x_3 - x_0 \\ y_1 - y_0 & y_2 - y_0 & y_3 - y_0 \\ z_1 - z_0 & z_2 - z_0 & z_3 - z_0 \end{bmatrix} + \frac{1}{6} \det \begin{bmatrix} x_1 - x_0 & x_3 - x_0 & x_4 - x_0 \\ y_1 - y_0 & y_3 - y_0 & y_4 - y_0 \\ z_1 - z_0 & z_3 - z_0 & z_4 - z_0 \end{bmatrix} \quad (3.14)$$

### 3.4.2 Stiffness of gas-filled cavity

The change in gas pressure and cavity volume is non-linear. To reach the solution the developed method had to use iteration to reach the solution. The stiffness of the system changes between every iteration and depend on the change in gas pressure due to volume change. To calculate the change in stiffness from the gas-filled cavity on the glass structure, the gas can be treated as a gas-spring coupled to the glass structure elements in each node facing the cavity. The equilibrium equation for a spring can be written as

$$F = k\delta \quad (3.15)$$

where  $F$  is the force acting on the spring,  $k$  is the spring stiffness and  $\delta$  is the deformation in the spring. When applying this to the IGU case, the force acting on the node is the gas pressure. The gas pressure was applied with the same amplitude in the whole cavity and was calculated with the change in cavity volume. Since each element had a different volume change the stiffness correlation can be seen as the change in gas pressure due to this element volume change. The change in gas pressure obtained in each element is non-linear but was linearized in each step of the iteration and can be expressed as

$$p_0 = \frac{\Delta p}{\Delta V(\delta)} V_0 \rightarrow \Delta p = \frac{p_0}{V_0} \Delta V(\delta) \quad (3.16)$$

where  $p_0$  is the initial gas pressure,  $V_0$  is the initial volume and  $\Delta V(\delta)$  is the change in element volume which depend on the displacement that occurred in the element.

The volume change,  $\Delta V$ , can be calculated for each element with the coordinates which defines the surface, the reference node and the displacement of the nodes. This is expressed with

$$\Delta V = -\frac{1}{6} \begin{bmatrix} x_0(y_4 - y_2) + x_2(y_0 - y_4) + x_4(y_2 - y_0) \\ x_0(y_1 - y_3) + x_1(y_4 - y_0) - x_3y_0 - x_4y_1 \\ x_0(y_2 - y_4) + x_2(y_4 - y_0) + x_4(y_0 - y_2) \\ x_0(y_3 - y_1) + x_1(y_0 - y_2) + x_2(y_1 - y_3) + x_3(y_2 - y_0) \end{bmatrix}^T \begin{bmatrix} u_1 \\ u_2 \\ u_3 \\ u_4 \end{bmatrix} \quad (3.17)$$

where the indexes is described in Figure 3.3. This vector, containing the coordinates, will further be called  $\mathbf{C}_0$ . Observe that  $\mathbf{C}_0$  is transpose.  $u$  denotes the displacement of the nodes and is defined by

$$\mathbf{u} = \mathbf{N}\mathbf{a} \quad (3.18)$$

where  $\mathbf{N}$  is the shape functions and  $\mathbf{a}$  is the global solution vector [9].

By expressing the coordinate vector as  $\mathbf{C}_0$  and the displacement according to Eq. (3.18), the volume change in Eq. (3.17) could be expressed with

$$\Delta V = \mathbf{C}_0 \mathbf{N} \mathbf{a} \quad (3.19)$$

The interaction between gas and structure can now be expressed by rewriting the spring equilibrium equation, Eq. (3.15), as

$$F = k\delta \rightarrow F = \frac{p_0}{V_0} \mathbf{C}_0 \mathbf{N} \mathbf{a} \quad (3.20)$$

Each node had an influence area of 1/4 of the element area. To adjust for this the stiffness had to be integrated over the region which the node influenced,

$$\mathbf{K}_b = \int_A \mathbf{N}^T \frac{p_0}{V_0} \mathbf{C}_0 dA \quad (3.21)$$

where  $A$  is the influence area.

The FE-expression in each node can with Eq. (3.20) and Eq. (3.21) be expressed as

$$\mathbf{K}_b \mathbf{a} = \mathbf{f} \quad (3.22)$$

where the solution vector,  $\mathbf{a}$  and the load vector  $\mathbf{f}$  is the same as the global solution vector and load vector. This means that the adjustment for interaction between the gas and the structure can be combined with the global equilibrium equation, Eq. (3.5), as

$$\mathbf{K} \mathbf{a} - \mathbf{K}_b \mathbf{a} = \mathbf{f} \rightarrow (\mathbf{K} - \mathbf{K}_b) \mathbf{a} = \mathbf{f} \quad (3.23)$$

where the stiffness matrix  $\mathbf{K}$  was the stiffness of the solid materials in the model which were modeled with linear elasticity as explained in Section 3.3.3.

The gas can be modeled as finite elements according to [16]. In [16] the non-linearity can be solved by calculating a tangential element stiffness for the gas elements and iterate the residual load vector of the system. But as earlier mentioned, more elements will lead to longer and more demanding calculations.

## 3.5 Abaqus

Abaqus is a computer software which is used to do FE-analysis. For the analysis in this thesis the specific software used is Abaqus CAE and Abaqus Standard. Abaqus CAE is an application used for creating models and analyze the results. The application has a user friendly interface with model visualization which makes it easy to use in pre-processing of the model as well as analyzing the results of the calculations. Abaqus Standard is the application which runs the calculations.

## 3.6 Calfem

Calfem is a FE-toolbox in the numerical computing program Matlab. Calfem is mainly used as a tool for teaching the finite element method. The program has been developed at the Division of Structural Mechanics, Lund University. Some of the functions used in Calfem is modified to either speed up the calculations or change the input and/or output of existing functions.

# Chapter 4

## IGU finite element modeling

### 4.1 Material and geometry

The model was defined in a 3-D space with the width of the IGU in x-direction, the height in y-direction and the depth in z-direction, as illustrated in Figure 4.1.

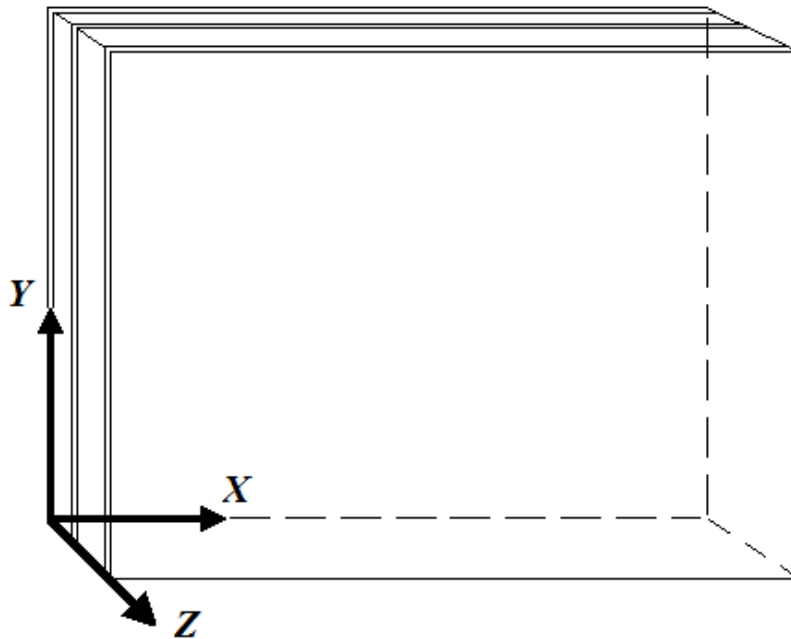


Figure 4.1: Definition of axis. The figure shows a model with 3 glass panes but the axis definition is the same for a model with 2 glass panes

The 3-D model consisted of two or three glass panes which were divided by a spacer. All the dimensions of the IGU could be changed but the geometry was restricted to a rectangular shape. The material properties of both the glass and the spacer could also be changed. The spacer was meshed to have different material properties so both the primary and secondary sealant could be given realistic material properties.

## 4.2 Elements and mesh

The glass was modeled with the 8 node solid-shell elements described in section 3.3.2

A 2D-mesh, shown in Figure 4.2, was first created of one glass surface. This mesh was copied in the z-direction to create a 3D-mesh of a glass pane. The second and third glass panes were created by copy the mesh for the first glass pane. The spacer was added by using the elements around the boundary of the glass panes.

Figure 4.2 shows that the rim of the glass pane had smaller elements. The reason for this was so that the spacer and secondary sealant could be modeled with separate material properties. A function were created to collect the elements and nodes which defined the cavity, these were used to calculate the cavity volume and apply the load.

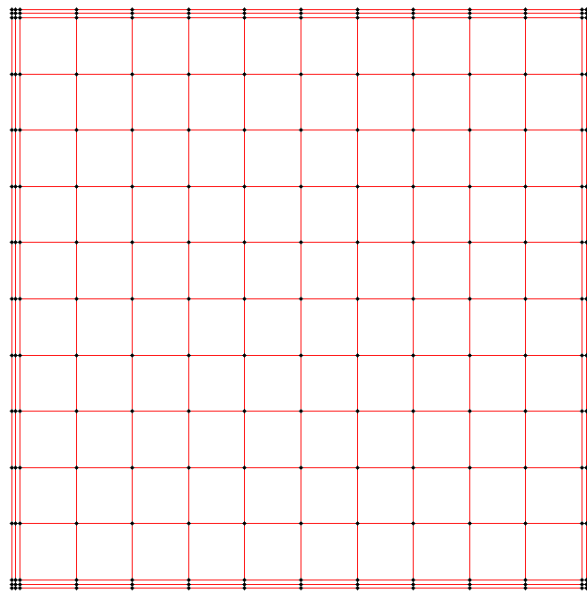


Figure 4.2: 2-D mesh of a 1.0x1.0 m glass pane.

## 4.3 Loads and boundary conditions

Boundary conditions were only prescribed for the nodes in the outer glass pane. The displacement of the four corner nodes were set to zero. To restrict any rigid body motions of the model in the three dimensional space, the bottom right corner was restricted in y- and z-direction and the top right corner was restricted in x- and z-direction.

The loads were applied as uniformly distributed loads over the surfaces of the glass panes acting lateral towards the surface.

## 4.4 Solution procedure

In the method the gas pressure induced by volume change was adjusted until the ideal gas law was fulfilled. The expression which the solution converge toward is

$$((p_{atm} + p_{gas,n})V)/(nR(T + \Delta T)) = 1 \quad (4.1)$$

where  $p_{gas,n}$  is the gas pressure difference from the initial value,  $p_{atm}$  and  $V$  is the cavity volume. If the expression in Eq. (4.1) was not fulfilled the iteration procedure continue and the residual is calculated with

$$res = 1 - ((p_{atm} + p_{gas,n})V)/(nR(T + \Delta T)) \quad (4.2)$$

By the residual, a new gas pressure can be calculated as

$$p_{gas,n+1} = p_{gas,n} + res(nR(T + \Delta T)/V) \quad (4.3)$$

where  $p_{gas,n+1}$  is the gas pressure which was applied as a new load in the cavity. The stiffness of the system is updated with regard to the volume change which is described in Section 3.4. With the new load and new stiffness the updated displacement and cavity volume can be calculated. This was repeated until Eq. (4.1) is fulfilled. A flow chart of the method is shown in Figure 4.3.

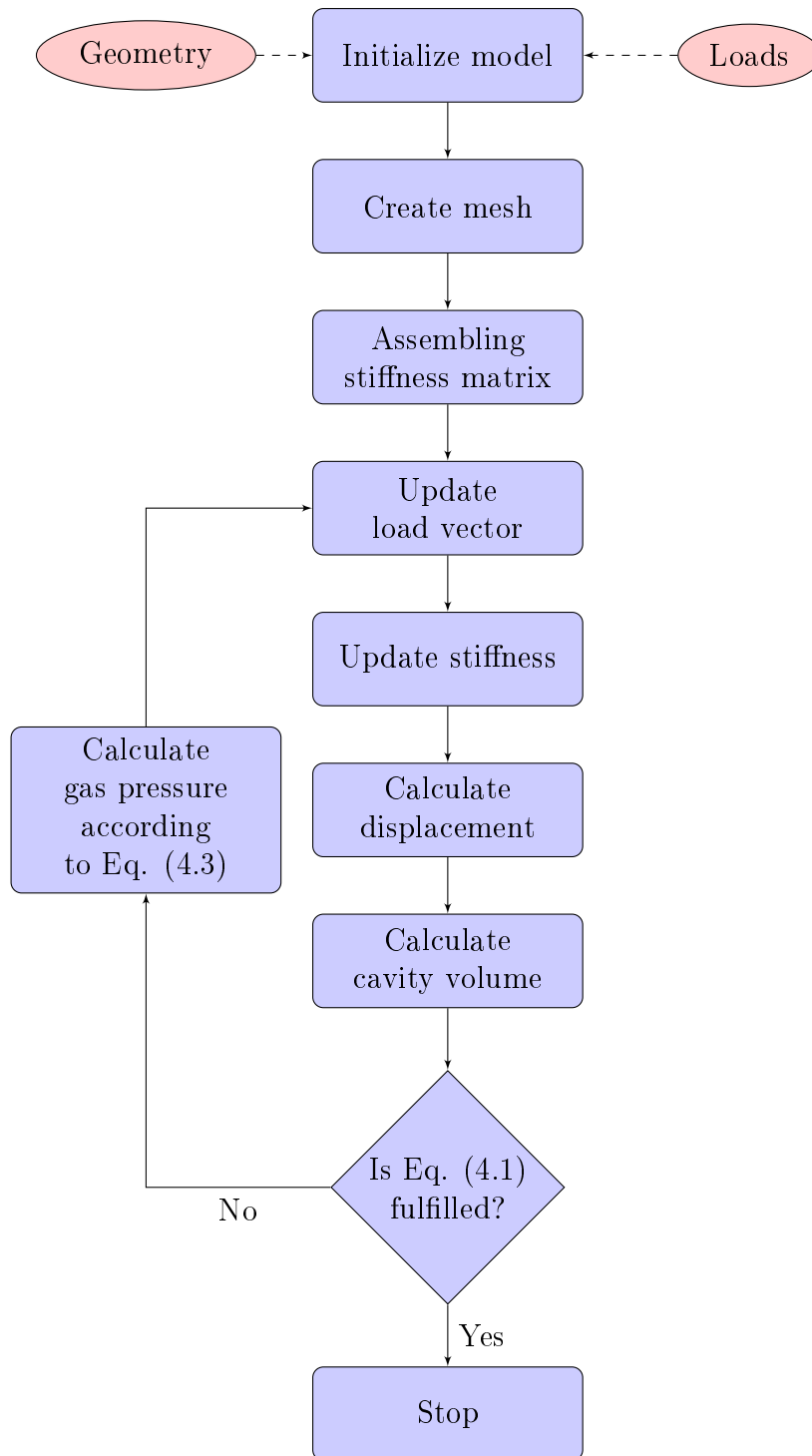


Figure 4.3: Flow chart of IGU FE program.

To speed up the calculations an error tolerance was set here to a value of  $1 \cdot 10^{-6}$ .

If the model with two cavities the same procedure was applied as for the model with one cavity. If the model only was exposed to temperature change and/or pressure change the both cavities would act in the same manor but if the model was exposed to wind load the method would iterate on the most depending cavity which in most cases should be the outer cavity. Loads and boundary conditions was applied in the same way as when only one cavity is modeled.

An alternative method was created which changed the gas pressure in each iteration step. The volume of the cavity was calculated in each step and the method checked the ideal gas law according to

$$(pV) - (nR(T + \Delta T)) = 0 \quad (4.4)$$

The pressure was then changed depending on if the expression in Eq. (4.4) were positive or negative. This method was not as effective as the first mentioned but the instability problem of the system, that is further explained in Section 4.4.1, was not a problem in this case. The amount of iterations needed for the method to converge were significantly larger than for the procedure which was used as the computational method.

#### 4.4.1 Instability problem

Since the cavity was small an instability problem occurred during the iteration procedure. This resulted in that even a small deformation would create a large pressure difference. This pressure difference created a large deformation and the system became unstable. To counteract this, the volume change was restricted to 10% between two iterations. This might lead to longer calculation time for some load cases but this was accepted because it was required for most models.

### 4.5 Implementation in Matlab

The method was implemented in Matlab using the FE-toolbox Calfem which consists of functions for FE-modeling.

In Calfem there is also a meshing tool to create 2-D meshes. This tool was used to mesh the outer surfaces of the first glass pane. The mesh tool gives a coordinate matrix for all the nodes, a vector with the degrees of freedom and a topology matrix which was used to assemble the stiffness matrix and the global vectors.

Calfem consists of functions needed for FE-analysis, for example a function to assemble the stiffness matrix and calculating the nodal forces. Other functions, such as a function to calculate volume change, were implemented.

### 4.6 IGU finite element modeling in Abaqus

#### 4.6.1 Purpose

Analysis of IGUs were also performed by use of the commercial FE-software Abaqus to verify the developed model. In this section the Abaqus model is described

## 4.6.2 Geometry and material

The geometry of the model were chosen according to Table 4.1. Since the Abaqus model was used to evaluate the developed method same geometry was chosen for the two models.

Table 4.1: Geometry of Abaqus model.

Glass thickness	4 mm
Cavity depth	16 mm
Spacer width	15 mm

The glass panes were modeled with the material parameters that is presented in Table 2.10. As for the developed model, the spacer was modeled with the material properties of glass.

When large displacements occur in a model, non-linear geometry may have to be accounted for. In non-linear simulations, calculations is made on the current geometry. The Abaqus model was analyzed with both linear and non-linear geometry for different loads and dimensions. When comparing with the developed method linear geometry was used. Non-linear geometry was used to evaluate the necessity of using large displacement.

### 4.6.2.1 Elements and mesh

The model was meshed with two types of elements, one type for the structure, glass pane and spacer, and one type for the gas within the cavity.

The elements used for the glass structure was an 8 node quadrilateral continuum shell element within Abaqus, called SC8R. This element has an underlying shell element in the calculations but is modeled as a 3-D element. The element uses first-order interpolation and reduced integration and can be used to calculate stress and displacement [19]. The SC8R allow two-sided contact which makes it suitable for modeling contact with hydrostatic volume elements. This is because the SC8R is a continuum shell element which is modeled as a hexahedron instead of a normal classic shell element which usually is modeled with its mid-surface geometry.

The gas-filled cavity was modeled with hydrostatic fluid elements which is a volume element in the cavity [17]. A reference node was created within the cavity and the volume element is defined by the surface of the cavity and the reference node. The element couples the deformation of the cavity and the pressure that is developed in the gas, that in turn is applied as a load on the boundary of the cavity [17].

The mesh of the model was created with a sweep mesh in Abaqus. Element size was 7.5 mm at the spacer and the mesh over the glass depended on the dimension of the model. The size of the element was 1/20 of the dimension of the glass. The width of the element was 1/20 the width of the glass and the height of the element was 1/20 the height of the glass.

The mesh of the Abaqus model is illustrated in Figure 4.4.

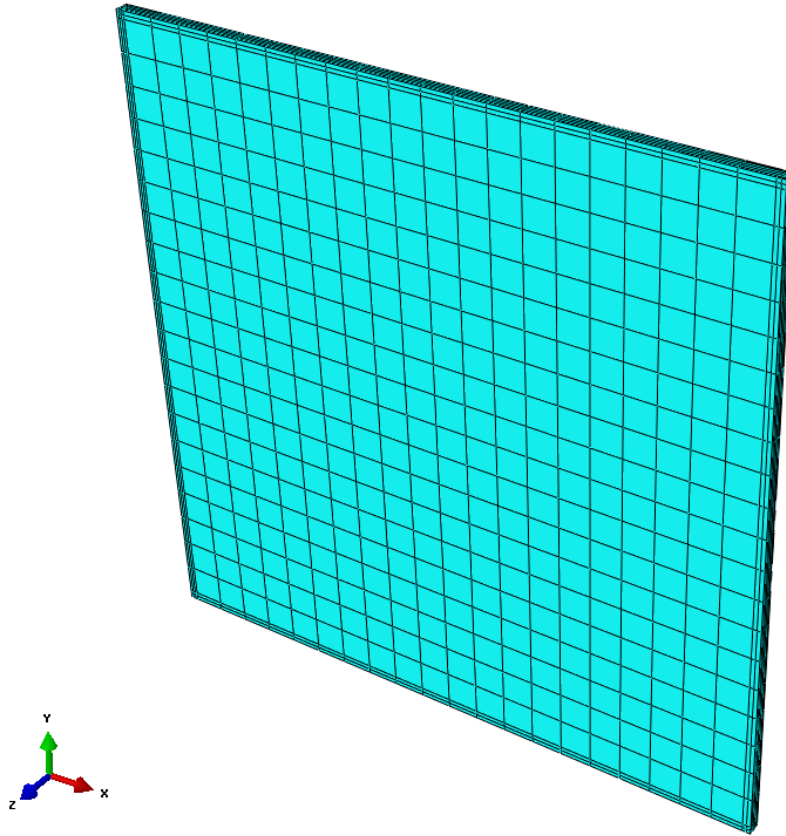


Figure 4.4: Mesh of Abaqus model.

### 4.6.3 Loads and boundary conditions

The wind load was applied as a uniformly distributed pressure on the outward surface of the glass pane. The pressure inside the cavity was applied as a uniformly distributed pressure towards all surfaces within the cavity. The pressure amplitude was the same in all directions.

A change in temperature of the gas was applied to the reference node within the cavity.

The model was restrained in four nodes in the same manner as the developed model. Table 4.2 shows which restrictions were applied in each node. The location of the nodes is shown in Figure 4.5. The prescribed boundary condition tells which direction the model was restricted to have any displacement.

Table 4.2: Boundary conditions applied in the Abaqus model.

Point	Prescribed boundary condition
1	x-, y- and z- direction
2	y- and z-direction
3	x- and z-direction
4	z-direction

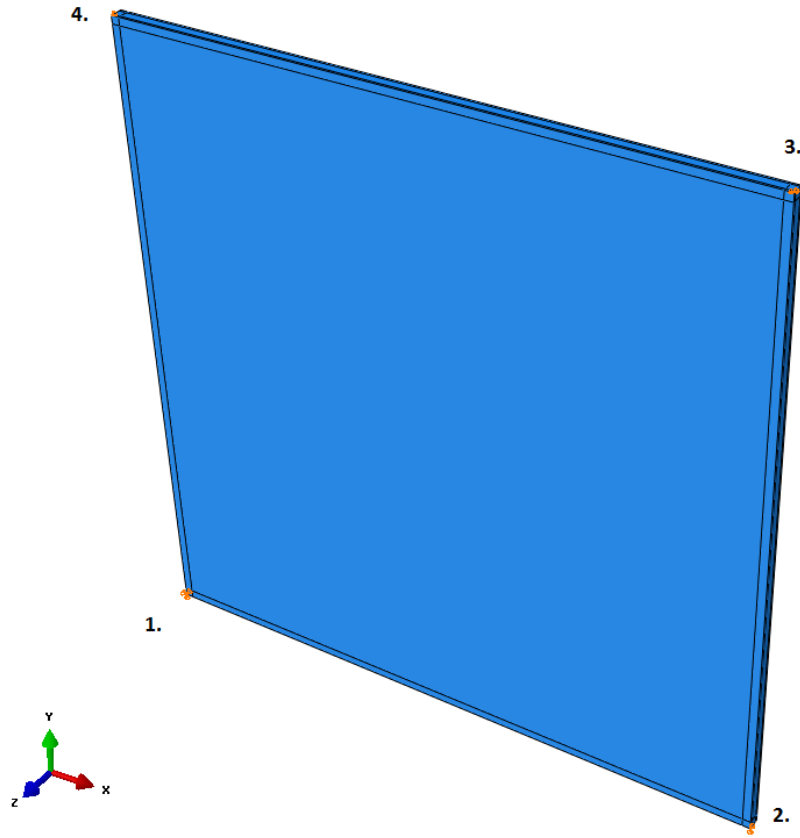


Figure 4.5: Boundary conditions applied in the Abaqus model.

# Chapter 5

## Numerical studies

### 5.1 Evaluation of the developed method

The developed model was compared to the model created in Abaqus. Analyzes were made for three different dimensions of the IGU as shown in Table 5.1. For each dimension three analyzes were made with change in atmospheric pressure, change in temperature and applied wind load.

Table 5.1: Dimensions of the glass pane.

0.6x0.6 $m^2$
1.2x1.2 $m^2$
1.8x1.8 $m^2$

The displacement and the maximum stresses in the glass were used for comparison between the Abaqus model and the developed model.

#### 5.1.1 Temperature change

For the load case when the IGU was subjected to a change in temperature the temperature change of the gas was prescribed. The gas temperature at the start of the analysis was set to 20° C, which is assumed to be the same as when the IGU were assembled. The temperature in the gas was then changed. The minimum and maximum gas temperature that the IGU were subjected to was -30° C and +40° C respectively.

Table 5.2 shows the maximum displacement developed in an IGU when the unit was subjected to temperature change from 20° C to -30° C. Figure 5.1 shows the maximum stress in a glass pane for an IGU with dimensions 1.8x1.8 when subjected to temperature change and Figure 5.2 shows the stress when the 0.6x0.6 m IGU was subjected to temperature change.

Table 5.2: Displacement of IGU subjected to temperature change 20° C to -30° C with different dimensions.

Dimensions [ $m^2$ ]	Max. total bulging [mm]		% -offset
	Calfem	Abaqus	
0.6x0.6	5.29	5.48	3.5
1.2x1.2	8.77	8.62	1.8
1.8x1.8	9.08	9.04	0.4

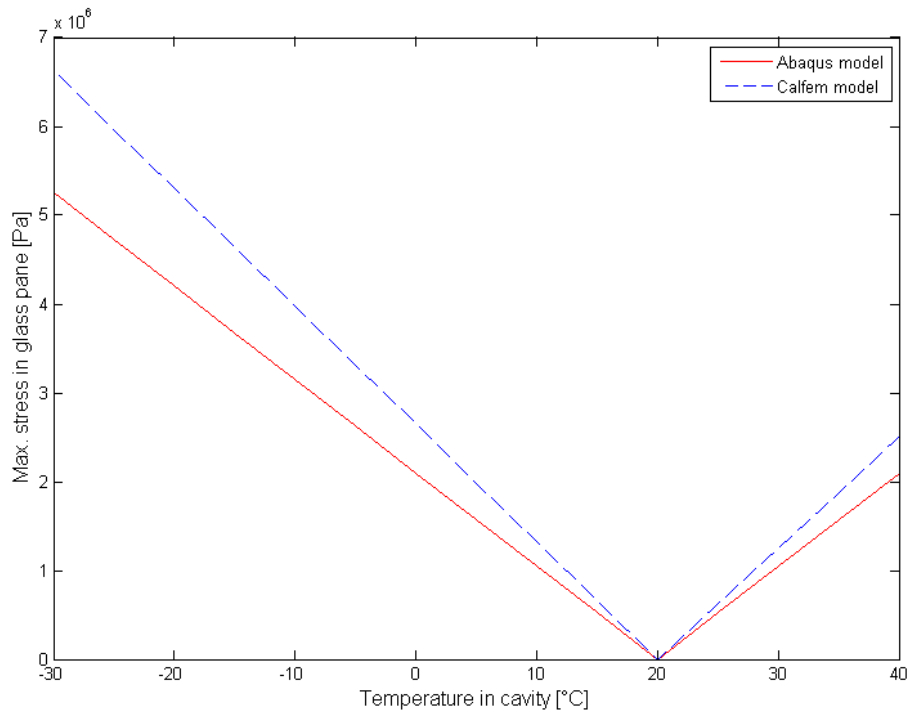


Figure 5.1: Maximum stress in glass pane with dimensions 1.8x1.8.

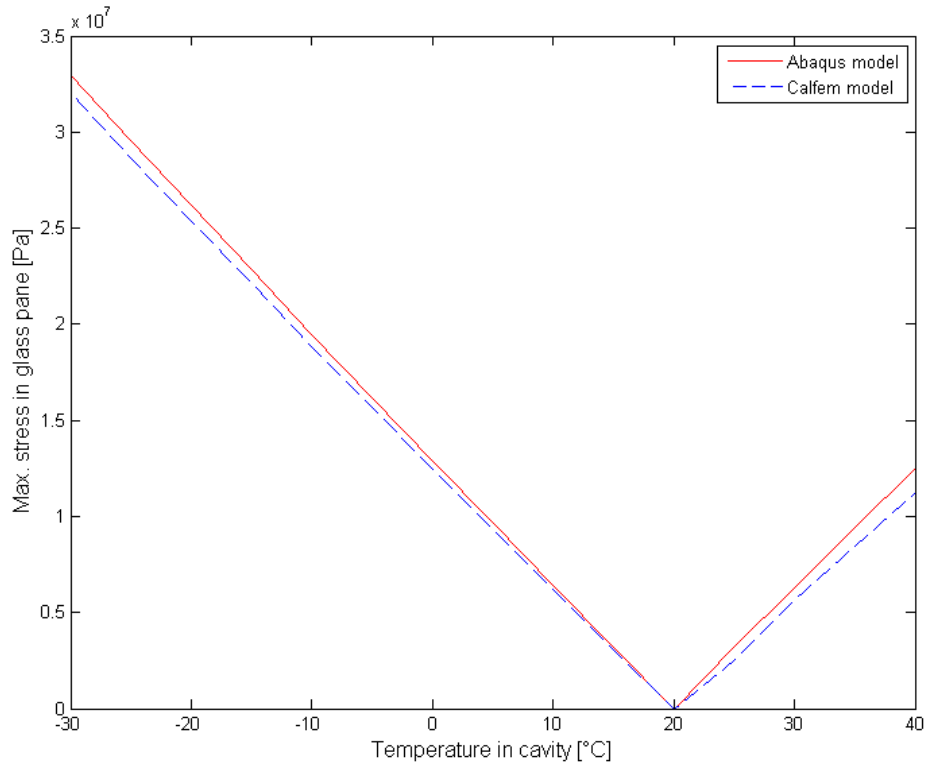


Figure 5.2: Maximum stress in glass pane with dimensions 0.6x0.6.

Figure 5.3 shows the displacement change with varying dimensions. The glass pane was square with varying dimensions so the x-axis shows both the width and height of the unit. The load applied in this case was a temperature change 20° C to -20° C.

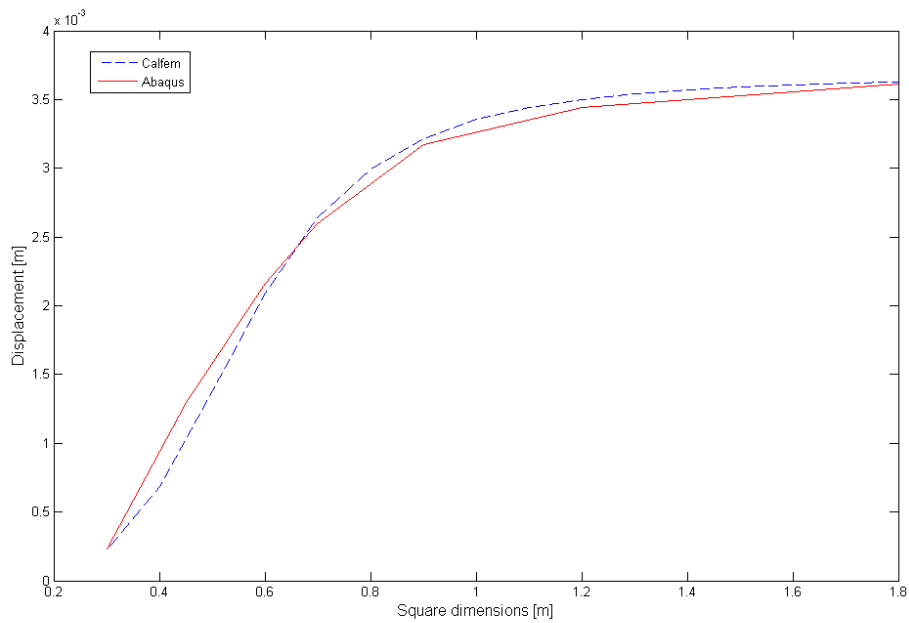


Figure 5.3: Change in displacement with varying dimensions.

### 5.1.2 Pressure change

For the analysis of pressure change the models were loaded with an increase or decrease of the atmospheric pressure by changing the gas pressure in the cavity. The pressure was changed from  $-3$  kPa to  $3$  kPa with steps of  $250$  Pa. Table 5.3 shows the maximum displacement developed in an IGU when the unit was subjected to an increase in gas pressure of  $3$  kPa.

Table 5.3: Displacement of IGU subjected to an increase in gas pressure of  $3$  kPa with different dimensions.

Dimensions [ $m^2$ ]	Max. total bulging [mm]		% -offset
	Calfem	Abaqus	
0.6x0.6	0.89	0.93	4.5
1.2x1.2	1.55	1.50	3.8
1.8x1.8	1.62	1.61	1.3

### 5.1.3 Wind load

The wind load was applied to the IGU by applying an outer pressure load on one of the panes. Large displacements developed in both the developed model and the Abaqus model. As shown in Figure 5.4 the difference between Abaqus and the developed model was very small. The figure shows the displacement of the outer and inner glass pane separately since the displacement differs between the two glass panes.

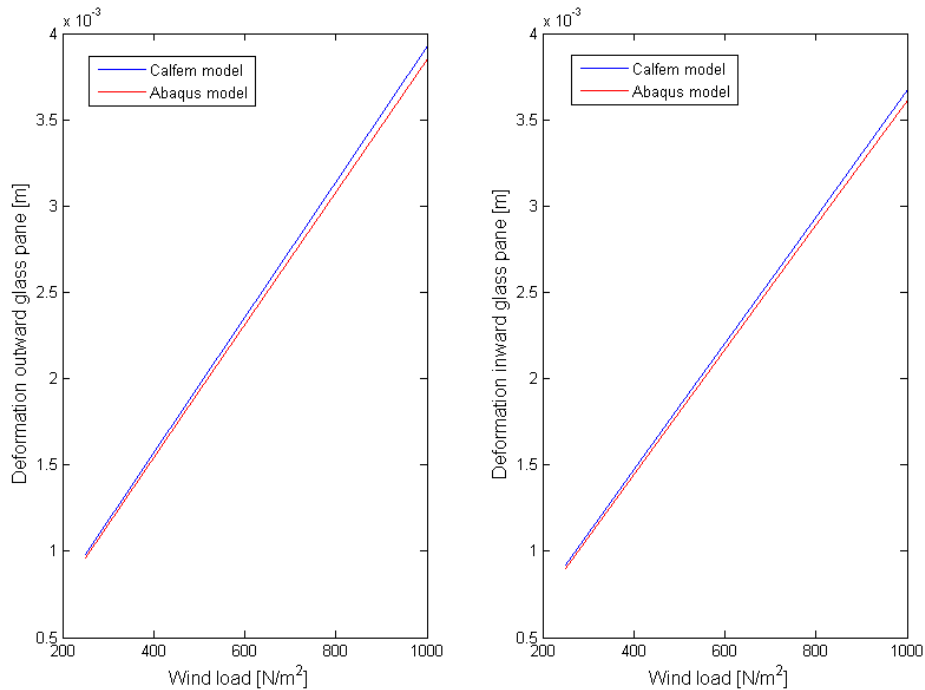


Figure 5.4: Displacement of outer and inner glass pane with dimensions  $1.2 \times 1.2$   $m^2$  subjected wind load.

### 5.1.4 Three glass IGUs

A number of analysis was performed for three glass IGUs. Comparisons were made between the developed model and the Abaqus model. The comparison of IGUs with three glass is shown in Table 5.4. The results in the table was for IGU with the dimensions  $1.2 \times 1.2 m^2$ . Table 5.5 shows the displacements of the outer and inner glass panes when the IGU was subjected to wind load.

Table 5.4: Displacement of IGU with three glass, with dimensions  $1.2 \times 1.2 m^2$  and different load cases.

Load case	Max. total bulging [mm]		% -offset
	Calfem	Abaqus	
Pressure diff.	2.97	2.94	1.2
Temperature change	13.49	12.50	7.9

Table 5.5: Displacement of IGU with three glass, with dimensions  $1.2 \times 1.2 m^2$  subjected to wind load.

Glass pane	Max. bulging [mm]		% -offset
	Calfem	Abaqus	
Outer	2.45	2.39	2.2
Inner	1.97	1.93	1.8

### 5.1.5 Non-linear geometry

Analysis were made including non-linear geometry in Abaqus. The comparison to the result with linear geometry is shown in Figure 5.5. The IGU was subjected to wind load and the dimensions was varied between  $0.2 \times 0.2 m^2$  to  $1.8 \times 1.8 m^2$ . The load amplitude was set to 1 kPa. The figure shows the displacement in the outer glass pane which was the one subjected to the load.

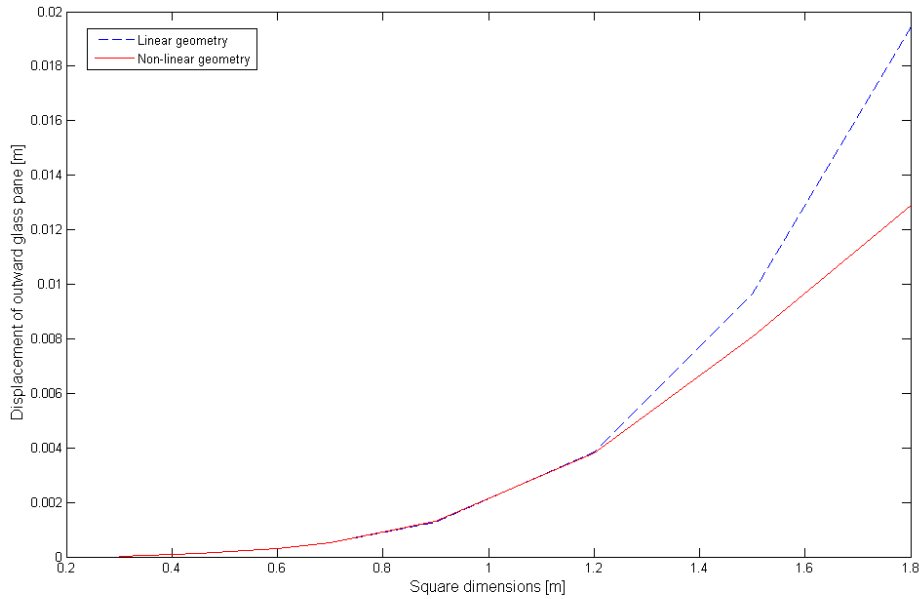


Figure 5.5: Comparison between linear and non-linear geometry in Abaqus when subjected to wind load with an amplitude of  $1 \text{ kPa}$ .

### 5.1.6 Discussion of evaluation

The difference between the Abaqus model and developed model was small. The difference in displacement varied between 0-8% between the two models. The models were created in a similar manner to enable good comparison. The boundary conditions were the same and the element size was almost equal between the models. The element type was different in the two models. With the results presented above the developed model were proved to be a good model for analyzing IGUs.

For the wind load case the displacement became large for both models when analyzing large glass dimensions. To make the method reliable for large dimensions and wind load, second order theory should be adapted. This means that the geometry is non-linear and should be updated between each iteration. As shown in Figure 5.5, non-linear geometry has a large impact on the displacement for IGUs with large dimensions and this must be added to the developed model.

## 5.2 Comparison with experimental data

In the comparison analysis of the developed model with experimental data, the input data described in Section 2.1 was used.

In [11] three different experimental tests were performed. In Test 1 the deformations of IGUs exposed to different temperatures on each side was measured. The temperature in the gas was linearly interpolated between the surfaces of the glass on both sides of the cavity. The temperature and pressure difference used in the Calfem analysis is presented in Table 5.6. In Test 2 the IGUs were exposed to  $-10.15^\circ \text{ C}$  on both sides and the

atmospheric pressure during the test was 101.6 kPa. The temperature during Test 3 was 20.9° C and the atmospheric pressure was 102.2 kPa.

Table 5.6: Conditions used in Calfem analysis.

IGU	Temperature outer cavity [°C]	Temperature inner cavity [°C]	Pressure difference [kPa]
1	-6.6	7.65	0.8
2	-7.9	9.15	0.5
3	-6.9	8.1	0.3
5	-7.4	12.45	0.2

The results of Test 1-Test 3 are presented in Table 5.7 - 5.9.

Table 5.7: Displacement of glass and the total bulging in the center of the glass pane from Test 1, Calfem analysis.

IGU	Displacement			Total bulging in middle [mm]
	Outer	Middle	Inner	
1	2.35	-3.05	-4.45	6.80
2	3.95	-1.12	-2.80	6.75
3	3.87	-1.11	-2.80	6.67
4	-	-	-	-
5	3.61	-1.29	-2.37	5.98

Table 5.8: Displacement of glass and the total bulging in the center of the glass pane from Test 2, Calfem analysis.

IGU	Displacement			Total bulging in middle [mm]
	Outer	Middle	Inner	
1	-	-	-	-
2	5.32	0	-5.32	10.63
3	5.03	-0.31	-4.82	9.85
4	2.95	0	-2.95	5.89
5	4.89	-0.24	-4.74	9.63

Table 5.9: Displacement of glass and the total bulging in the center of the glass pane from Test 3, Calfem analysis.

IGU	Displacement			Total bulging in middle [mm]
	Outer	Middle	Inner	
1	0.32	-0.29	-0.73	1.04
2	0.53	0	-0.53	1.06
3	0.50	-0.03	-0.48	0.99
4	0.26	0	-0.26	0.51
5	0.49	-0.03	-0.47	0.96

The results from the developed method was compared to the experimental results in [11]. In the developed model, the displacement in each of the glass panes was calculated but only the displacement at the surfaces were measured in the experimental analysis. Table 5.10 shows the results from the Calfem analysis and the result obtained in [11]. Table 5.11 shows the difference between the Calfem model and the result that was obtained in [11]. In Table 5.10 the difference between Test 1 and Test 3, and Test 2 and Test 3 are shown. The reason for this was to neglect the residual deformations which were obtained in the experimental analysis in Test 3.

Table 5.10: Comparison between Calfem model and experimental results, [11].

IGU	Comparison of tests	Calfem [mm]	Abaqus [mm]	Measured Caliper [mm]
1	Test 1-Test 3	5.76	5.4	4.6
2	Test 1-Test 3	5.69	5.9	5.1
	Test 2-Test 3	9.57	10.3	9.4
3	Test 1-Test 3	5.68	5.1	4.3
	Test 2-Test 3	8.87	8.4	6.3
4	Test 2-Test 3	6.41	7.4	8.3
5	Test 1-Test 3	5.02	5.6	5.6
	Test 2-Test 3	8.67	8.5	8.2

Table 5.11: Difference between developed model and experimental results, [11].

IGU	Comparison of tests	Calfem-Abaqus [mm]	Calfem - Caliper [mm]
1	Test 1-Test 3	0.36	1.16
2	Test 1-Test 3	-0.21	0.59
	Test 2-Test 3	-0.73	0.17
3	Test 1-Test 3	0.58	1.38
	Test 2-Test 3	0.47	2.57
4	Test 2-Test 3	-0.99	-1.89
5	Test 1-Test 3	-0.58	-0.58
	Test 2-Test 3	0.17	0.47

The difference between the developed model and the results from the experimental test and the Abaqus analysis is presented in Table 5.12, where the total bulging for each test is compared.

Table 5.12: Difference between results from developed model, the experimental analysis and the Abaqus analysis.

<b>Test 1</b>	<b>Offset [mm]</b>	
<b>IGU</b>	<b>Calfem-Caliper</b>	<b>Calfem-Abaqus</b>
1	-2.00	0.56
2	-4.05	-0.25
3	-4.43	0.75
4	-	-
5	-4.22	-0.46
<b>Test 2</b>	<b>Offset [mm]</b>	
<b>IGU</b>	<b>Calfem-Caliper</b>	<b>Calfem-Abaqus</b>
1	-	-
2	-4.47	-0.78
3	-3.25	0.59
4	-5.61	-2.26
5	-3.17	0.29
<b>Test 3</b>	<b>Offset [mm]</b>	
<b>IGU</b>	<b>Calfem-Caliper</b>	<b>Calfem-Abaqus</b>
1	-3.26	0.21
2	-4.64	0
3	-5.82	0.14
4	-2.69	-0.26
5	-3.64	0.12

### 5.2.1 Discussion of comparison analysis

As shown in Table 5.12 there was a difference of 2-5 mm between the developed model and the experimental results and a difference of 0-2 mm between the developed method and the Abaqus model. In [11] it was concluded that the Abaqus model differed approximately 2-5 mm from the measured value which was close to the result from the developed model.

The difference between the result from the Abaqus model in [11] and the developed model may differ from both input data and how the glass panes were meshed.

When bulging occur in the glass panes the heat transfer through the IGU changes. The heat flux is dependent on the distance it travels through a medium. When bulging occurs this distance changes and this lead to a change in heat transfer through the IGU. This will affect the insulating capacity of the IGU and should be considered in the analysis.

As mentioned in [11] the residual deformations in the IGU was fairly large and they recommended further studies of this. This will effect the results of the experimental test and this was not accounted for in the result or the model.



# Chapter 6

## Discussion and further work

### 6.1 Discussion

A method for calculating the bulging of IGUs was developed and implemented in Calfem. The method was able to analyze IGUs subjected to wind load, temperature change and change in gas pressure. The method was compared with analyzes in Abaqus and the difference in displacement between the developed method and the simulations in Abaqus was small for all load cases.

The dimensions of the IGU and the material properties can easily be modified in the developed method. The elements used in the method is good to analyze different kinds of glass, for example laminated glass. The method was created to handle simple glass panes but should easily be able to change to a different set up.

The method was fairly fast and the calculations only took a few seconds. The method had to restrict the volume change between each iteration because of the instability problem described in Section 4.4.1. Because of this the method had to do more iterations to reach the result. The number of iterations varies between 10-30 depending on dimensions and loads. Larger dimensions and larger loads demands more iterations. Optimizations of the method could probably lower the number of iterations needed and then also lower the computational time even further.

Non-linear geometry was neglected in the Calfem model due to lack of time. Non-linear geometry is recommended when analyzing larger dimensions subjected to wind load due to the large deformation that develops.

What happens in the spacer was not considered at all, there might be plastic deformations forming when the large loads are applied. When constructing the method the spacer and sealant were modeled as glass but when comparing with [11] the spacer and sealant were set to more realistic material properties.

The boundary condition was chosen to be similar to [11]. This was a decent choice when examining pressure difference and temperature change since the pressure within the cavity counteract the load and almost no displacement develops over the edge between the corners. When the IGU was subjected to wind load the pressure within the cavity will not counteract this displacement and a displacement occurs over the edge. A better choice of boundary condition was to restrict any movement along the entire edge of the unit. When analyzing temperature change and pressure change the difference in displacement

was small between the two choices of boundary condition but it will have a huge impact when analyzing wind load.

## 6.2 Conclusion

The main goal of the thesis was to create a computational method which were able to calculate displacement and stress in an IGU.

A computational method were established using the FE-method. The IGU were modeled in 3D and subjected to various loads such as wind load, temperature change and change in gas pressure. The method was able to analyze IGUs with different dimensions and material properties. To find the solution, the developed method calculated the cavity volume and used the ideal gas law to update the gas pressure. The gas pressure were obtained by the residual of the ideal gas law and the method could find the solution by iterations.

The results from the developed method were compared to simulations in Abaqus and the results in [11]. The developed method gave acceptable results and showed the behavior of an IGU and an approximation of the stress and displacement that occur.

## 6.3 Further work

The method should be able to consider non-linear geometry. This is especially needed when large IGUs are exposed to wind load since large displacements develops. Experimental analysis of IGUs exposed to lateral load would be interesting to analyze since large displacements occur in the glass panes.

The spacer was simplified in the model and further analysis of its influence should be carried out. The stiffness of the spacer and the stress which it endure during loading could be interesting to analyze. If plastic deformation occur in the spacer this should be accounted for in the analysis.

Since the insulating capacity is important to analyze when designing an IGU, a FE-model of the heat transfer through the IGU should be integrated in the method. That would give more accurate temperatures through the IGU and assure that the IGU can achieve the insulating capacity desired. A heat transfer model could possibly also be used to analyze the effect that bulging has on the heat transfer through the IGU.

# Bibliography

- [1] Burström P. G., *Byggnadsmaterial*. 2006, Lund, Studentlitteratur.
- [2] Carlsson P. O., *Bygga med glas*. 2005, Stockholm, Glasbranschföreningen.
- [3] Carlsson P. O., *Glas - Möjligheternas byggnadsmaterial*. 1992, Stockholm, Statens råd för byggnadsforskning.
- [4] Guardian Europa S.á r.l. Dudenlang, *Glass Time technical manual*. 2012, Luxembourg, Guardian mkt.
- [5] Van der Bergh S. et al., *Window spacer and edge seals in insulating glass units: A state-of-the-art review and future perspectives*. 2012, Elsevier B.V..
- [6] Wolf A.T., *Studies into the life-expectancy of insulating glass units*. 1998, France, RILEM Publications SARL.
- [7] Haldimann M. et al., *Structural Use of Glass*. 2008, Zürich, IABSE-AIPC-IVBH.
- [8] SMHI, <http://www.smhi.se/kunskapsbanken/meteorologi/lufttryck-1.657>, 2015-03-25.
- [9] Ottosen Saabye N. and Petersson H., *Introduction to the Finite Element Method*. 1992, Lund, Prentice Hall.
- [10] Ottosen Saabye N. and Ristinmaa M., *The Mechanics of Constitutive Modeling*. 2005, Lund, Elsevier.
- [11] Andersson M. and Nilsson S., *Bulging of insulating glass units - Numerical and experimental analysis*. 2014, Lund, Division of Structural Mechanics,LTH.
- [12] Jönsson G., *Fysik i vätskor och gaser*. 2010, Lund, Teach Support.
- [13] Isaksson T. Mårtensson A., *Byggekonstruktion - Regel- och formelsamling*. 2010, Lund, Studentlitteratur
- [14] Guardian Russia, <http://www.guardian-russia.ru/en/about-glass/modern-technologies/float-glass-production-technology/>, visited 2015-04-13.
- [15] Austrell P-E. et. al., *Calfem - A finite element toolbox version 3.4* 2004, Lund, Division of Structural Mechanics,LTH.
- [16] Fulton K. and Schmidt R., *Finite Elements in Analysis and Design - A two-dimensional ideal gas finite element*. 2001, Wyoming, Elsevier.

- [17] Abaqus 6.12 SIMULIA, *Abaqus Theory Manual - 3.8.1 Hydrostatic fluid calculations*, [http://www.maths.cam.ac.uk/computing/software/abaqus\\_docs/docs/v6.12/](http://www.maths.cam.ac.uk/computing/software/abaqus_docs/docs/v6.12/), visited 2015-05-07.
- [18] Abaqus 6.12 SIMULIA, *Abaqus Analysis User's Manual - 11.5.1 Surface-based fluid modeling* [http://www.maths.cam.ac.uk/computing/software/abaqus\\_docs/docs/v6.12/](http://www.maths.cam.ac.uk/computing/software/abaqus_docs/docs/v6.12/), visited 2015-05-07.
- [19] Abaqus 6.12 SIMULIA, *Abaqus Analysis User's Manual - 29.6.2 Choosing a shell element*, [http://www.maths.cam.ac.uk/computing/software/abaqus\\_docs/docs/v6.12/](http://www.maths.cam.ac.uk/computing/software/abaqus_docs/docs/v6.12/), visited 2015-05-07.
- [20] Hautekeer J.-P et al., *Key factors governing technologies on the growing China Insulating Glass Market*, Dow Corning.
- [21] Fröling M., *Strength design methods for glass structures*, 2013, Lund, Division of Structural Mechanics,LTH.
- [22] Cardoso R.P.R et. al., *Enhanced assumed strain (EAS) and assumed natural strain (ANS) methods for one-point quadrature solid-shell elements - International Journal for Numerical Methods in Engineering (75) 156-187*, 2008, John Wiley & Sons, Ltd.
- [23] Berry, D.T. & Yang H.T.Y, *Formulation and Experimental Verification of a Pneumatic Finite Element - International Journal for Numerical Methods in Engineering (39): 1097-1114*, 1996, John Wiley & Sons, Ltd.
- [24] Velchev D. & Ivanov I.V., *A finite element for insulating glass units - Challenging Glass 4 & COST Action TU0905 Final Conference*, 2014, Bulgaria, Taylor & Francis Group.

# Appendix A

## Matlab code

### A.1 Main program

```
close all
clear all
% -----
% Iteration options
% -----
TOL = 1e-6;
% -----
% -----
% Loads
% -----
q_temp = 0000;
p_temp = 000;
Ttot_1 = 273.15-30;
%
Ttot_2 = 273.15-20; % Neglect if only one cavity is analyzed
%
% -----
% NUMBER OF CAVITIES
nbr_cav = 1;
% -----
% Cavity properties
% -----
% Atmospheric pressure
patm = 101325;
% thickness of the space between the glass
cav_d_1 = 0.016;
%
cav_d_2 = 0.016; % Neglect if only one cavity is analyzed
%
% Intitial temperature
T0 = 293.15;
% -----
% -----
% GLASS
% -----
% Thickness of glass
t_1 = 0.004;
```

```

t_2 = 0.004;
%
t_3 = 0.004; % Neglect if only one cavity is analyzed
%
% Width of glass pane
width = 1.8;
% Height of glass pane
height = 1.8;
% Youngs module
E = 73e9;
% Poisson's ratio
v = 0.22;
% spacer thickness
t_spacer = 0.015;
% Density glass
rho = 2500;
% -----
% -----
% MESH
% -----
[Vertices,Segments,Surfaces,Segp,mp] = pane_mesh2D(width,height,t_spacer);
[Coord,Edof,Dof,meshdb] = strMeshgen(Vertices,Segments,Surfaces,Segp,mp);
% 3-D MESH
if nbr_cav == 1
    Coord3d = [Coord(:,1), Coord(:,2), zeros(length(Coord),1);...
              Coord(:,1), Coord(:,2), ones(length(Coord),1)*t_1;...
              Coord(:,1), Coord(:,2), ...
              ones(length(Coord),1)*(t_1+cav_d_1);...
              Coord(:,1), Coord(:,2), ...
              ones(length(Coord),1)*(t_1+t_2+cav_d_1)];

    Dof3d = [Dof; Dof + max(Dof(:));...
            Dof + 2*max(Dof(:)); Dof + 3*max(Dof(:))];

    Edof3d = [Edof(:,1), Edof(:,2:13), Edof(:,2:13) + max(Edof(:));...
             Edof(:,1) + max(Edof(:,1)),...
             Edof(:,2:13) + 2*max(Edof(:)),...
             Edof(:,2:13) + 3*max(Edof(:))];

    % Add spacer
    spacer_el = [...
                 extrSurf(1,meshdb); extrSurf(2,meshdb); extrSurf(3,meshdb);...
                 extrSurf(4,meshdb); extrSurf(5,meshdb); extrSurf(6,meshdb);...
                 extrSurf(7,meshdb); extrSurf(8,meshdb)];
    spacer_dofs = [Edof3d(spacer_el,14:25)...
                  Edof3d(spacer_el+length(Edof),2:13)];

    Edof3d = ...
            [Edof3d; [(1:length(spacer_dofs))'+max(Edof3d(:,1)) spacer_dofs]];
else
    Coord3d = [Coord(:,1), Coord(:,2), zeros(length(Coord),1);...
              Coord(:,1), Coord(:,2), ones(length(Coord),1)*t_1;...
              Coord(:,1), Coord(:,2), ...
              ones(length(Coord),1)*(t_1+cav_d_1);...
              Coord(:,1), Coord(:,2), ...
              ones(length(Coord),1)*(t_1+t_2+cav_d_1);...
              Coord(:,1), Coord(:,2), ...
              ones(length(Coord),1)*(t_1+t_2+cav_d_1+cav_d_2);...
              Coord(:,1), Coord(:,2), ...

```

```

ones (length(Coord),1)*(t_1+t_2+t_3+cav_d_1+cav_d_2)];

Dof3d = [Dof; Dof + max(Dof(:)); Dof + 2*max(Dof(:));...
        Dof + 3*max(Dof(:)); Dof + 4*max(Dof(:));...
        Dof + 5*max(Dof(:))];

Edof3d = [Edof(:,1), Edof(:,2:13), Edof(:,2:13) + max(Edof(:));...
        Edof(:,1) + max(Edof(:,1)),...
        Edof(:,2:13) + 2*max(Edof(:)), Edof(:,2:13) + 3*max(Edof(:));
        Edof(:,1) + 2*max(Edof(:,1)),...
        Edof(:,2:13) + 4*max(Edof(:)),...
        Edof(:,2:13) + 5*max(Edof(:))];
% Add spacer
spacer_el = [...
    extrSurf(1,meshdb); extrSurf(2,meshdb); extrSurf(3,meshdb);...
    extrSurf(4,meshdb); extrSurf(5,meshdb); extrSurf(6,meshdb);...
    extrSurf(7,meshdb); extrSurf(8,meshdb)];

spacer_dofs = [Edof3d(spacer_el,14:25)...
    Edof3d(spacer_el+length(Edof),2:13);...
    Edof3d(spacer_el+length(Edof),14:25)...
    Edof3d(spacer_el+2*length(Edof),2:13)];

Edof3d = [...
    Edof3d; [(1:length(spacer_dofs))'+max(Edof3d(:,1)) spacer_dofs]];
end

% Coordinates
[Ex,Ey,Ez] = coordxtrKP(Edof3d,Coord3d,Dof3d,mp(2));

%
spacer_mem = zeros(length(spacer_el),1);
spacer_mem2 = [1 5 6 7 8 9 10 11 12 13 14.....
    28 39 40 41 42 43 44 45 46 47 48.....
    52 63 64 65 66 67 68 69 70 71 72.....
    75 77 79 81 83 85 87 89 91 93 95]';
for i = 1:length(spacer_mem2)
    spacer_mem(spacer_mem2(i)) = spacer_mem2(i);
end
if nbr_cav == 2
    spacer_mem = [spacer_mem; spacer_mem];
end

% Ref node
if nbr_cav == 1
    ref_node_1 = [width/2,height/2,t_1+cav_d_1/2];
    ref_node_2 = [0,0,0];
else
    ref_node_1 = [width/2,height/2,t_1+3*cav_d_1/4];
    ref_node_2 = [width/2,height/2,t_1+t_2+cav_d_1+cav_d_2/4];
end

% Cavity elements and nodes
if nbr_cav == 1
    [cav_el,cav_dofs,nel_cav,cav_el_tmp]=...
        cavitymesh(meshdb,Edof,Edof3d,Ex,Ey,width,height,t_spacer);
else
    [cav_el,cav_dofs,nel_cav,cav_el_tmp]=...

```

```

        cavitymesh(meshdb,Edof,Edof3d,Ex,Ey,width,height,t_spacer,1);
end

% Cavity volume
% Cavity 1
if nbr_cav == 1
    vol_init_1 = cav_vol(nel_cav,ref_node_1,Ex,Ey,Ez,cav_el,cav_el_tmp);
    vol_init_2 = 0;
else
    vol_init_1 = cav_vol(nel_cav/2,ref_node_1,Ex,Ey,Ez,...
        [cav_el(1:(nel_cav-length(cav_el_tmp))/2);...
        cav_el(nel_cav-length(cav_el_tmp)+1:...
        (nel_cav-length(cav_el_tmp)/2)],...
        cav_el_tmp(1:length(cav_el_tmp)/2,:));
    % Cavity 2
    vol_init_2 = cav_vol(nel_cav/2,ref_node_2,Ex,Ey,Ez,...
        [cav_el((nel_cav-length(cav_el_tmp))/2+1:...
        (nel_cav-length(cav_el_tmp)));...
        cav_el((nel_cav-length(cav_el_tmp)/2)+1:nel_cav)],...
        cav_el_tmp(length(cav_el_tmp)/2+1:length(cav_el_tmp),:));
end

% Ideal gas law
% Cavity 1
nRT_1 = vol_init_1*patm;
nR_1 = nRT_1/T0;
% Cavity 2
nRT_2 = vol_init_2*patm;
nR_2 = nRT_2/T0;

% -----
% -----
% Initial
% -----
% nbr dofs
ndof = max(Edof3d(:));
nel = length(Ex);
% ep = [ir rho], ir = integration points
ep = [3 rho];
%
D = hooke(4,E,v);
%
eq = [0 0 0];

% -----
% -----
% Boundary conditions
% -----
% corner_dofs = [extrPoint(1,meshdb) extrPoint(4,meshdb)...
%     extrPoint(7,meshdb) extrPoint(10,meshdb)];
% bc = [corner_dofs(:,1) zeros(3,1);
%     corner_dofs([2,3],2) zeros(2,1);
%     corner_dofs([1,3],3) zeros(2,1);
%     corner_dofs(3,4) zeros(1,1)];
tempvecspace = [1 2 3 4 5 6 7 8 9 10 11 12];
bc = [extrSeg(tempvecspace,meshdb,[1,2,3])...
    zeros(length(extrSeg(tempvecspace,meshdb,[1,2,3])),1)];
bc = [bc; [extrSeg(tempvecspace,meshdb,[1,2,3])+675....
    zeros(length(extrSeg(tempvecspace,meshdb,[1,2,3])),1)]];

```

```

bc = [bc; [extrSeg(tempvecspace, meshdb, [1, 2, 3])+675*2.....
        zeros(length(extrSeg(tempvecspace, meshdb, [1, 2, 3])), 1)]];
bc = [bc; [extrSeg(tempvecspace, meshdb, [1, 2, 3])+675*3.....
        zeros(length(extrSeg(tempvecspace, meshdb, [1, 2, 3])), 1)]];
% -----
% -----
% Iteration
% -----
% -----
% Assembling
% -----
K = sparse(ndof, ndof);
% for i = 1:nel
%     [Ke, ~]=m_ress_PD_mod2(Ex(i, :), Ey(i, :), Ez(i, :), ep, D);
%     K = sparse_assem(Edof3d(i, :), K, Ke);
% end
for i = 1:nel-nbr_cav*length(spacer_el)
    [Ke, ~]=m_ress_PD_mod2(Ex(i, :), Ey(i, :), Ez(i, :), ep, D);
    K = sparse_assem(Edof3d(i, :), K, Ke);
end
D_spacer1 = hooke(4, 2.9*width*1e9, 0.3);
D_spacer2 = hooke(4, 1.6e6, 0.2);
for i = 1:nbr_cav*length(spacer_el)
    j = i + nel - nbr_cav*length(spacer_el);
    if spacer_mem(i) > 0
        [Ke, ~]=m_ress_PD_mod2(Ex(j, :), Ey(j, :), Ez(j, :), ep, D_spacer1);
    else
        [Ke, ~]=m_ress_PD_mod2(Ex(j, :), Ey(j, :), Ez(j, :), ep, D_spacer2);
    end
    K = sparse_assem(Edof3d(j, :), K, Ke);
end
% -----
% Load
% -----
p_T_step_1 = (Ttot_1-T0)*nR_1/vol_init_1;
p_T_step_2 = (Ttot_2-T0)*nR_2/vol_init_2;
f_q = zeros(ndof, 1);
f_e = zeros(ndof, 1);
eq_wind = q_temp;
eq_dp = p_temp;

% Assembling load vector
% Wind
for i = 1:length(Edof)
    [fe_wind]=flw2i4e_mod(Ex(i, 1:4), Ey(i, 1:4), 2, eq_wind);
    f_q(Edof3d(i, 4), 1) = f_q(Edof3d(i, 4), 1) + fe_wind(1);
    f_q(Edof3d(i, 7), 1) = f_q(Edof3d(i, 7), 1) + fe_wind(2);
    f_q(Edof3d(i, 10), 1) = f_q(Edof3d(i, 10), 1) + fe_wind(3);
    f_q(Edof3d(i, 13), 1) = f_q(Edof3d(i, 13), 1) + fe_wind(4);
end

f_q = ...
    cav_press(Ex, Ey, cav_el, cav_dofs, nel_cav, ...
    cav_el_tmp, eq_dp, eq_dp, f_q, nbr_cav);

p_init_1 = patm + p_T_step_1;
p_init_2 = patm + p_T_step_2;
vol_cav_1 = vol_init_1;

```

```

vol0_cav_1 = vol_cav_1;
vol_cav_2 = vol_init_2;
vol0_cav_2 = vol_cav_2;
delta_p_1 = 0;
delta_p_2 = 0;
iter = 3;
a = zeros(ndof,1);
x = 0;

vol_diff_1 = 0.1;
my_ctrl_1 = 0;
vol_diff_2 = 0.1;
my_ctrl_2 = 0;

while abs(1-iter) > TOL
    x = x + 1;
    % Load vector for gas pressure
    f_e = zeros(ndof,1);
    f_e = cav_press(Ex,Ey,cav_el,cav_dofs,nel_cav,...
        cav_el_tmp,delta_p_1,delta_p_2,f_e,nbr_cav);
    % Stiffness matrix from change in pressure
    Kb = sparse(ndof,ndof);
    if nbr_cav == 2
        Kb = gasstiffmat(Kb,Ex,Ey,cav_el,cav_dofs,nel_cav,...
            cav_el_tmp,patm,delta_p_1,vol_init_1,ref_node_1,...
            delta_p_2,vol_init_2,ref_node_2);
    else
        Kb = gasstiffmat(Kb,Ex,Ey,cav_el,cav_dofs,nel_cav,cav_el_tmp,...
            patm,delta_p_1,vol_init_1,ref_node_1);
    end
    R = f_q + f_e;
    R(bc(:,1)) = 0;
    R0 = R;
    Ktot = K - Kb;
    [da,r] = solveq(Ktot,R,bc);

    Ed = extract(Edof3d,da); %

    % -----
    % Volume
    % -----
    itemp = 1;
    tempX = Ex; tempY = Ey; tempZ = Ez;
    for i = 1:8
        tempX(:,i) = Ex(:,i) + Ed(:,itemp);
        tempY(:,i) = Ey(:,i) + Ed(:,itemp+1);
        tempZ(:,i) = Ez(:,i) + Ed(:,itemp+2);
        itemp = itemp+3;
    end
    check_lrg_def_1 = 0; check_lrg_def_2 = 0;
    if nbr_cav == 1
        for i = 1:196
            for j = 1:8
                if tempZ(i,j) > t_1 + cav_d_1/2
                    tempZ(i,j) = t_1 + cav_d_1/2;
                    check_lrg_def_1 = 1;
                end
                if tempZ(196+i,j) < t_1 + cav_d_1/2

```

```

        tempZ(196+i, j) = t_1 + cav_d_1/2;
        check_lrg_def_1 = 1;
    end
end
end
else
    for i = 1:length(Edof)
        for j = 1:8
            if tempZ(i, j) > t_1 + 3*cav_d_1/4
                tempZ(i, j) = t_1 + 3*cav_d_1/4;
                check_lrg_def_1 = 1;
            end
            if tempZ(length(Edof)*2+i, j) < ...
                t_1 + t_2 + cav_d_1 + cav_d_2/4;
                tempZ(length(Edof)*2+i, j) = ...
                t_1 + t_2 + cav_d_1 + cav_d_2/4;
                check_lrg_def_2 = 1;
            end
            if tempZ(i+196, j) < tempZ(i, j)
                tempZ(i+196, j) = tempZ(i, j);
            elseif tempZ(i+196, j) > tempZ(i+196*2, j)
                tempZ(i+196, j) = tempZ(i+196*2, j);
            end
        end
    end
end
end

% Cavity volume

% Cavity volume
% Cavity 1
if nbr_cav == 2
    vol_cav_1 = cav_vol(nel_cav/2, ref_node_1, tempX, tempY, tempZ, ...
        [cav_el(1:(nel_cav-length(cav_el_tmp))/2); ...
        cav_el(nel_cav-length(cav_el_tmp)+1:...
        (nel_cav-length(cav_el_tmp)/2))], ...
        cav_el_tmp(1:length(cav_el_tmp)/2, :));

    if check_lrg_def_1 == 1
        vol_cav_1 = ...
            4*(cav_d_1*(width-2*t_spacer)*(heigth-2*t_spacer)/2)/3;
    end
    [vol_cav_1, my_ctrl_1, vol_diff_1, vol0_cav_1] = ...
        vol_iter(vol_cav_1, vol0_cav_1, my_ctrl_1, vol_diff_1);
    %
    % Cavity 2
    vol_cav_2 = cav_vol(nel_cav/2, ref_node_2, tempX, tempY, tempZ, ...
        [cav_el((nel_cav-length(cav_el_tmp))/2+1:...
        (nel_cav-length(cav_el_tmp)));...
        cav_el((nel_cav-length(cav_el_tmp)/2)+1:nel_cav)], ...
        cav_el_tmp(length(cav_el_tmp)/2+1:length(cav_el_tmp), :));

    if check_lrg_def_2 == 1
        vol_cav_2 = ...
            4*(cav_d_2*(width-2*t_spacer)*(heigth-2*t_spacer)/2)/3;
    end
    [vol_cav_2, my_ctrl_2, vol_diff_2, vol0_cav_2] = ...

```

```

        vol_iter(vol_cav_2,vol0_cav_2,my_ctrl_2,vol_diff_2);

    iter = abs((patm+delta_p_1)*vol_cav_1 / (nR_1*Ttot_1));
    iter_2 = abs((patm+delta_p_2)*vol_cav_2 / (nR_2*Ttot_2));

    delta_p_1 = delta_p_1 + (1-iter)*(nR_1*Ttot_1)/vol_cav_1;
    delta_p_2 = delta_p_2 + (1-iter_2)*(nR_2*Ttot_2)/vol_cav_2;
else
    % Cavity volume
    vol_cav_1 =...
        cav_vol(nel_cav,ref_node_1,tempX,...
            tempY,tempZ,cav_el,cav_el_tmp);

    if check_lrg_def_1 == 1
        vol_cav_1 =...
            4*(cav_d_1*(width-2*t_spacer)*(heigth-2*t_spacer)/2)/3;
    end
    %
    [vol_cav_1,my_ctrl_1,vol_diff_1,vol0_cav_1] =...
        vol_iter(vol_cav_1,vol0_cav_1,my_ctrl_1,vol_diff_1);
    iter = abs((patm+delta_p_1)*vol_cav_1 / (nR_1*Ttot_1));
    delta_p_1 = delta_p_1 + (1-iter)*(nR_1*Ttot_1)/vol_cav_1;
end
end
outward = max(abs(Ed(141,:)))
if nbr_cav == 2
    middle = max(abs(Ed(141+196,:)))
    inward = max(abs(Ed(141+196*2,:)))
else
    inward = max(abs(Ed(141+196,:)))
end
%pcav = patm*(vol_init/cav_vol-1)+abs(p_T_step)
delta_p_1
delta_p_2

vol_cav_1
vol_cav_2

% Stress calculations

SN1=zeros(ndof,1); % Normal stress vector
SS1=zeros(ndof,1); % Shear stress vector
TT1=zeros(ndof,1); % Smoothing vector

% Loop over number of element of the glass pane
for i=1:length(Ex(1:nel-length(spacer_el),1))
    [sn,ss,es,et,eci]=ress_s3(Ex(i,:),Ey(i,:),Ez(i,:),D,ep(1),Ed(i,:));
    SN1=vec_assem(Edof3d(i,:),SN1,sn); % Assembling normal stresses to nodes
    SS1=vec_assem(Edof3d(i,:),SS1,ss); % Assembling shear stresses to nodes
    % Assembling the smoothing vector
    TT1=vec_assem(Edof3d(i,:),TT1,ones(3*8,1));
end

SN1=SN1./TT1; % Smoothed normal stresses
SS1=SS1./TT1; % Smoothed shear stresses
% Fixing possible NaN and Inf problems

```

```

for i = 1:length(SN1),
    if TT1(i,1) == 0,
        SN1(i,1) = 0;
    end
end

SS1=SS1./TT1; % Smoothed shear stresses
% Fixing possible NaN and Inf problems
for i = 1:length(SS1),
    if TT1(i,1) == 0,
        SS1(i,1) = 0;
    end
end

%Calculation of stress
Maxprincsig1 = []; % Maximum principal stresses, corresponding to layer 2
for i = 1:3:ndof,

    S = [SN1(i,1) SS1(i,1) SS1(i+1,1);
          SS1(i,1) SN1(i+1,1) SS1(i+2,1);
          SS1(i+1,1) SS1(i+2,1) SN1(i+2,1)]*(10^(-6));
    eigenval = eigs(S);
    maxprincsig1 = max(eigenval);
    Maxprincsig1 = [Maxprincsig1;maxprincsig1];
end
tmpi = 1;
for i = 1:1 + nbr_cav
    max(SN1(tmpi:(tmpi+674)*2))
    tmpi = tmpi + 675;
end

```